



The University of
Nottingham

UNITED KINGDOM · CHINA · MALAYSIA

DEPARTMENT OF CIVIL ENGINEERING

NOTTINGHAM GEOSPATIAL INSTITUTE

JAMMING OF GPS & GLONASS SIGNALS

**A study of GPS performance in
maritime environments under jamming
conditions, and benefits of applying
GLONASS in Northern areas under such
conditions**

AUTHOR	OEYSTEIN GLOMSVOLL
SUPERVISOR	DR XIAOLIN MENG
DATE	24 SEPTEMBER 2014

Project thesis submitted in part fulfilment of the requirements for the degree of
Master of Science in Positioning and Navigation Technology, The University of
Nottingham.

Abstract

Growing dependence on Global Navigation Satellite System (GNSS), especially GPS, for positioning and navigation at sea has raised a concern about the potential risks of signal interference. Technology for jamming is easily available, and in recent years there have been many cases of intentional jamming.

As GPS is the principal means of position fixing used by the Norwegian Navy, important questions to find answers to is how vulnerable the GPS and the Electronic Chart Display and Information System (ECDIS) are to a jamming attack, and further whether employing the Glonass satellite system in addition to GPS will provide better performance regarding robustness and redundancy when receivers are exposed to jamming. By having a Coast Guard Vessel operating inshore the Norwegian fjords as case, this research aims to explore these issues and it does so by asking the following research questions:

- Will employing Glonass in addition to GPS provide better performance in Northern areas when the systems are exposed to GNSS jammers?
- How is the ability of the existing GPS system on board a Norwegian Coastguard Vessel to provide a reliable position when there is a jamming threat, and how will the ECDIS system on board handle an eventually loss of GPS position?

The study consists of two jamming tests: A static test where focus is to analyze and compare the GPS and Glonass system and a dynamic test where the GPS and ECDIS system on board is analyzed when exposed to jamming.

The results from the static test showed that the jammer has effect on large distances, and that the different receivers used react differently when exposed to jamming. Further, the carrier-to-noise ratios for Glonass are less affected by the jammer, and the receiver is able to track Glonass satellites with lower carrier-to-noise ratios than GPS satellites. We have seen that utilizing Glonass satellites in addition to GPS satellites in the receiver contribute to a later loss of position fix and an earlier calculation of new position under difficult jamming conditions.

The dynamic test showed that the marine grade GPS receiver is easy to jam. A weak jamming signal caused the GPS receivers to give misleading information without any warning from itself or the ECDIS system. The ECDIS system provided an adequate DR positioning, but there are issues that need to be resolved for better functionality.

As Glonass signals has shown to be more resistant to jamming than GPS signals, applying the Glonass system in addition to GPS might provide benefits with regards to reliability and redundancy, especially for maritime navigation in Northern areas where the Glonass satellites also have higher elevation and better coverage than GPS.

Acknowledgment

I want to express my gratitude to all who have been involved in this research project.

To make the fieldwork possible I especially want to thank Captain Sverre Aas and his crew on board the Norwegian Coast Guard Vessel “Farm”. Without their cooperation and contribution to both the static and dynamic jamming test the fieldwork would not have been possible to carry out.

Thanks to my colleagues for constructive discussion.

Thanks to technician Sean Ince and researcher Lukasz Boneberg at the Nottingham Geospatial Institute who have gathered equipment and given assistance of setting it up, and have provided support in analyzing the data.

Dr Xiaolin Meng has provided guidance and supervised the project, thanks for all help and feedback.

Finally I wish to thank my partner Nina and my newborn son Eivind for their help and understanding during the writing of this thesis.

Nottingham 23. September 2014,

Øystein Glomsvoll.

Contents

Abstract.....	1
Acknowledgment	3
Figures and Tables	6
1 Introduction	8
1.1 Background	8
1.2 Research Aim	9
1.3 Research objectives	10
1.4 Thesis outline	10
2 Literature review.....	12
2.1 Overview of Global Navigation Satellite Systems (GNSS)	12
2.1.1 Signal Structure GPS.....	12
2.1.2 Signal structure Glonass.....	14
2.1.3 Signal power.....	15
2.2 Influences on GNSS measurements.....	16
2.3 Radio frequency interference	17
2.3.1 Characterization of jamming signals.....	18
2.3.2 Classification of jamming devices and their signal characteristics	18
2.3.3 Jamming effects on signal processing.....	20
2.3.4 Carrier-to-noise ratio	21
2.4 Research on GNSS jamming.....	24
2.4.1 Receivers ability to determine position	24
2.4.2 Jammer-to-signal ratios	25
2.4.3 Carrier-to-noise ratios.....	27
2.4.4 In-band and out-of-band jamming.....	28
2.4.5 Jamming of GPS and Galileo	29
2.4.6 Effect of solar radio emission interference on Glonass reception.....	31
2.5 Maritime GPS and jamming	32
2.6 Conclusion.....	34
3 Methodology.....	36
3.1 Methodology part 1: Jamming of static receivers	36
3.1.1 Scope	36
3.1.2 Equipment.....	36
3.1.3 Test setup.....	38

3.1.4 Procedure.....	38
3.1.5 Data-analysis techniques	39
3.1.6 Presentation of results.....	40
3.1.7 Research design issues and limitations.....	40
3.2 Methodology part 2: Jamming of dynamic receivers	42
3.2.1 Scope.....	42
3.2.2 Equipment and test setup.....	43
3.2.3 Procedure.....	44
3.2.4 Data analysis techniques.....	44
3.2.5 Presentation of results.....	45
3.2.6 Research design issues and limitations.....	45
4 Results and Discussion	46
4.1 Static Jamming Test	46
4.1.1 Satellite coverage.....	46
4.1.2 Carrier-to-noise ratios.....	47
4.1.3 Carrier-to-noise ratios at GPS L2.....	51
4.1.4 The first trial.....	52
4.1.5 The second and third trial	57
4.1.6 Comparison of the first trial versus simulator jamming tests.....	59
4.1.7 Discussion.....	60
4.2 Dynamic jamming test	63
4.2.1 Trial 1: Jamming effects on the GPS receivers.....	63
4.2.2 Trial 2: Jamming effects on the GPS receivers.....	67
4.2.3 Trial 2: Jamming effects on ECDIS.....	68
4.2.4 Discussion.....	71
5 Conclusion.....	73
6 Recommendations	74
7 Reference List.....	75
Appendices.....	78
Appendix A: Specifications Leica GS10 and AS10	78
Appendix B: Specifications Furuno GP90.....	79

Figures and Tables

Figure 2.1: Power spectra of GPS signals on L2 and L1 (Misra & Enge 2012).....	13
Figure 2.2: GNSS Frequency allocation (Navipedia 2014).....	14
Figure 2.3: Factors impacting GNSS performance (Norwegian Space Center 2013)	17
Figure 2.4: Signal characteristics for a group 1 jammer (Mitch et al. 2011).....	19
Figure 2.5: Spectrum of CW (1) and broadband jammer (2) (Kraus et al. 2011)	20
Figure 2.6: Processing gain of spread spectrum vs. narrowband RFI (Misra&Enge 2012)	21
Table 2.1: The ability of GPS receivers to resist jamming (Niekerk & Combrinck 2012)	25
Figure 2.7: The effect of various jammers on GPS receivers (Jones 2011).....	26
Figure 2.8: C/N ₀ for Ipex SW Receiver and the theoretical curve (Bauernfeind et al. 2011) .	27
Figure 2.9: Accuracy for Ipex SW Receiver (Bauernfeind et al. 2011)	28
Figure 2.10: C/N ₀ as a function of interference power level (Craven et al. 2013).....	29
Figure 2.11: C/N ₀ loss by four receivers when processing GPS L1 C/A (Borio et al. 2013)	30
Figure 2.12: Average C/N ₀ loss for GPS and Galileo signals (Borio et al. 2013).....	31
Table 2.2: Jamming effects observed on the Pole Star vessel in 2008 (Grant et al. 2010)....	33
Figure 3.1: Leica GS10 receiver and Leica AS10 antenna	37
Figure 3.2: Garmin etrex 20 receiver	37
Figure 3.3: L1 frequency jammer (SkyDec)	37
Figure 3.4: Map of the Site.....	38
Figure 3.5: Photo taken from the position of the receivers (point D)	39
Figure 3.6: The Norwegian Coast Guard Vessel “Farm”	42
Figure 3.7: Furuno GP90 receiver (www.furuno.com)	43
Figure 3.8: Furuno GPA019-S antenna.....	43
Figure 3.9: The splitter and Leica GS10 receiver.....	44
Figure 4.1: Skyplot GPS and Glonass satellites	47
Figure 4.2: C/N ₀ for two GPS satellites (G25 and G02) and distance to jammer vs time.....	48
Figure 4.3: C/N ₀ for G25 and R10 (high elevation satellites)	49
Figure 4.4: C/N ₀ for G04 and R02 (low elevation satellites).....	50
Table 4.1: C/N ₀ values for GPS SV and Glonass SV.....	50
Figure 4.5: C/N ₀ for GPS satellite G25 on L1 and L2.....	51
Figure 4.6: Trial 1: C/N ₀ GPS satellites	53
Figure 4.7: Trial 1: C/N ₀ Glonass satellites	53
Figure 4.8: Trial 1: Average loss in C/N ₀ for GPS and Glonass satellites	54
Figure 4.9: Trial 1: Horizontal Precision	56

Figure 4.10: Trial 1: Height Precision	56
Figure 4.11: Trial 1: Number of GPS and Glonass SV tracked and HDOP	57
Figure 4.12: Trial 2: Horizontal Precision	58
Figure 4.13: Trial 3: Horizontal Precision	58
Table 4.2: Distance to jammer when loss of position and obtaining new position fix.....	59
Figure 4.14: Average C/N_0 loss for GPS and Glonass vs distance to jammer.....	60
Figure 4.15: Skyplot GPS satellites.....	63
Figure 4.16: Carrier-to-noise ratios GPS satellites	64
Figure 4.17: Number of GPS satellites tracked by Leica and Furuno receiver.....	65
Figure 4.18: Position plot provided by the three receivers (Trial 1)	66
Figure 4.19: Position plot provided by the three receivers (Trial 2)	67
Figure 4.20: Position plot provided by the three receivers (Trial 2).....	68
Figure 4.21: NMEA inputs to the ECDIS	68
Figure 4.22: Alarm list on ECDIS.....	69
Figure 4.23: EPFS (Electronic Position Fixing System) alarm on AIS	69
Figure 4.24: Screenshot ECDIS (Trial 2).....	70

1 Introduction

1.1 Background

Growing dependence on Global Navigation Satellite System (GNSS), especially GPS, for positioning, navigation and timing (PNT) has raised a concern about the potential risks of signal interference, and since Volpe (2001) informed that GPS is in a very high grade vulnerable to intentional and unintentional interference, the awareness of the vulnerability of GPS has been a great issue and large concern.

The British QinetiQ study from the same year also states that the UK is growing more reliant on GPS for fundamental activities. The report says that “the fundamental weakness and vulnerabilities of GPS signal reception should be more widely publicized, especially for those services where significant inconvenience or critical impact could occur” (QinetiQ 2001:6). One such service is maritime navigation, and the report points to that GPS and differential GPS are used extensively for Maritime applications and in the case of loss of GPS signal the navigators have to revert to traditional means as radar, charts or dead reckoning (ibid).

Navigation News has stated that “GNSS systems (particularly GPS) have become the mariners’ primary navigation aid, and many vessels have no other means of navigation” (Navigation News Nov/Dec 2013:16). GNSS systems used on vessels are stand-alone or primarily augmented by differential GNSS. As GNSS signals are very weak and travel long distances before they reach the earth, they are vulnerable to all sources of interference which can be accidental and deliberate jamming, spoofing and unintentional interference. Many systems on a modern bridge are built around and very reliant on GNSS, and the implications of GNSS failure could be dramatically (Grant et al. 2009).

A Norwegian study (Norwegian Space Center 2013) has also been carried out to analyze the vulnerability of GNSS for critical infrastructure in Norway. The report supports the findings from Volpe (2001) and QinetiQ (2001) and highlights that the risk of intentional radio frequency interference with GNSS signals is an issue that should be taken seriously. The risk of intentional interference is considered to be

high mainly due to the widespread availability of low-cost and simple jamming equipment and the report recommends users who directly or indirectly depend on GNSS for positioning, navigation and precise timing to analyze the level of risk and implement relevant mitigation measures as required.

In recent years there have been many cases of intentional jamming, and the technology for jamming is easily available. A lot of research has been conducted with regards to jamming equipment and jamming of GPS, and when it comes to maritime navigation especially Grant et al. (2010) claim that there is a need for a more resilient GNSS for PNT, and emphasize that the terrestrial navigation system eLoran¹ would be the best solution. There has however been limited research on jamming of the Russian GNSS system, Glonass, which is today full operational on an equal basis as GPS.

1.2 Research Aim

As GPS is the principal means of position fixing used by all classes of mariner in ocean and coastal navigation important question to find answer to are how vulnerable the GPS and the electronic chart display and information system (ECDIS) on a Coast Guard Vessel operating inshore the Norwegians fjords are to a jamming attack? A study was therefore conducted on board the Norwegian Coast Guard Vessel "Farm".

Further, as we know that GPS is vulnerable and eLoran not yet is available, it would be of interest to investigate if there are some benefits of utilizing the Glonass system in addition to GPS for navigation applications when there is a threat of jamming. Although Glonass provides better satellite coverage in Northern sea areas, there are no Norwegian military vessels benefiting from this system. An important aim of this research is therefore to find out if Glonass utilized together with GPS is able to provide better redundancy and robustness when the GNSS receivers are exposed to jamming.

¹ Enhanced Long Range Navigation

1.3 Research objectives

The objective of this thesis is to analyze the performance of standalone static L1 C/A code GPS and combined GPS + Glonass receivers in tracking and acquisition mode when exposed to a jammer. As Norwegian Coast Guard Vessels normally utilize only the GPS system for navigation this research is conducted in order to investigate if employing the Glonass satellite system in addition to GPS will provide better robustness and redundancy, especially for maritime navigation in Northern areas where there potentially could be a jamming threat. When measuring performance the carrier-to-noise ratios of the signals from each satellite system will be of main focus.

Further, to assess the navigation system on board, the existing marine grade GPS receiver and chart system on board the Coast Guard Vessel will be investigated when it is affected by the same jammer. To assess the performance of this receiver it will be compared to a survey grade and consumer grade receiver.

The research questions are therefore:

- Will employing Glonass in addition to GPS provide better performance in Northern areas when the systems are exposed to GNSS jammers?
- How is the ability of the existing GPS system on board a Norwegian Coastguard Vessel to provide a reliable position when there is a jamming threat, and how will the ECDIS system on board handle an eventually loss of GPS position?

1.4 Thesis outline

Chapter 2, the literature review, gives a brief overview of the signal structure of GPS and Glonass, and further defines radio frequency interference and characterizes jamming signals. Typical classification of jamming devices and their signal characteristics will be studied. Further, jamming effects on signal processing in the receivers will be discussed, and there will be a focus on jammers' influence on carrier-to-noise ratios. Relevant research on GNSS jamming will be discussed and the last part of the literature review will cover jamming in a maritime setting.

Chapter 3 describes the methods applied for this research. First the methods for the static jamming test are discussed and then the methods for the dynamic jamming test on board the Coast Guard Vessel are described. The scope for each part will be presented and the chapter further covers the equipment used, the test setup, the procedure, and the data-analysis techniques. The way the results in the following chapter are presented will be described and research design issues and limitations will be discussed.

Chapter 4 consists of the results and a discussion part. The static jamming test is first covered with focus on carrier-to-noise ratios and precision in the code solution of the different receivers. A comparison of this live jamming test to a simulator jamming test is further made. The dynamic jamming test is then discussed with focus on the jammer's effects on the GPS receivers and the performance of the ECDIS when it lost its position input from the GPS.

Chapter 5 presents a conclusion to the static and dynamic jamming test, and Chapter 6 gives recommendations for further work.

2 Literature review

The literature review will give a brief overview of the GNSS systems with focus on GPS and Glonass. It will further study interference and look at the jamming signal from handheld devices which are currently easily available on internet and what effect those signals have on the GNSS signals and receivers. Moreover, there will be a closer look at some earlier research on how jamming can degrade the GNSS, especially with focus on the carrier-to-noise ratios, and in the end look at two trials that have been carried out by GLA² to see how jamming can influence maritime applications.

2.1 Overview of Global Navigation Satellite Systems (GNSS)

Today there are two operational global navigation satellite systems, the United States` GPS and the Russian Glonass. China is on their way on expanding its regional Beidou and the European Union has its own system Galileo under development. A common term of these satellite systems with global coverage is GNSS, and the systems work in approximately the same way (Hofmann-Wellenhof 2008).

2.1.1 Signal Structure GPS

All GPS satellites transmit continuous signals on the same two center frequencies L1 (1575.42 MHz) and L2 (1227.60 MHz). One signal for civilian users (Standard Positioning Service – SPS) and one encrypted signal for users authorized by the US Department of Defense are transmitted on L1, and the signal intended for authorized user is also transmitted on L2. The signal structure for SPS is public and described in detail in “Interface specification IS-GPS-200E” (Global Positioning Systems Wing 2010).

Although each satellite uses the same carrier frequencies they are modulated by a unique binary ranging code. This is the pseudorandom noise (PRN) code where the SPS codes for civilian users are called C/A (coarse/acquisition) code and the PPS codes for authorized users are the P(Y) codes. The C/A-code consists of a sequence of 1023 bits (chips) and is emitted at the frequency 1.023 MHz which repeats itself every millisecond. The P(Y)-code is a very long 10.23 MHz PRN- code and has a

² The General Lighthouse Authorities of the United Kingdom and Ireland.

period of one week. As the wavelength for the P(Y) code is shorter than the C/A-code, the precision in range measurement is better (Bingley 2013).

In addition to the carrier and ranging codes, GPS transmits a 50 Hz binary navigation data message (20ms bit duration). The navigation message has the following information: GPS time, satellite clock offset, satellite status and health, satellite ephemeris data and almanac which contains coarse orbit and status information for all satellites and data related to error corrections. The L1 carrier transmits the C/A-code, P(Y)-code and the navigation message, and the L2 carrier transmits the P(Y)-code and navigation message. The transmission scheme is called CDMA (Code Division Multiple Access) which is a form of spread spectrum. This technique allows differentiating between the satellites although they transmit on the same frequencies (Bingley 2013).

Direct Sequence Spread Spectrum (DS-SS) is used to spread the bandwidth and energy of the signal. The C/A-code is spread mainly over a 2 MHz wide frequency band and the P(Y) code is spread over about 20 MHz, all centered at the carrier frequency which is shown in Figure 2.1. The power spectral density is then reduced while the signal power is unchanged.

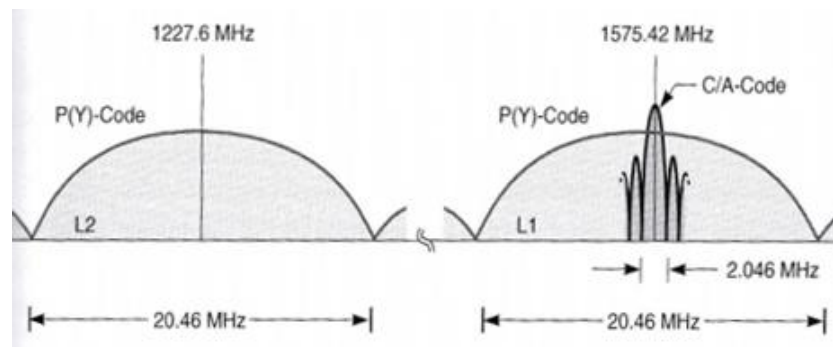


Figure 2.1: Power spectra of GPS signals on L2 and L1 (Misra & Enge 2012)

The three primary reasons for using DS-SS in satellite navigation (Kaplan & Hegarty 2006:115) are:

- *“The frequent phase inversions in the signal introduced by the PRN waveform enable precise ranging by the receiver.*

- The use of different PRN sequences enables multiple satellites to transmit signals simultaneously and at the same frequency. A receiver can distinguish among these signals based on their different codes. For this reason, the transmission of multiple DS-SS signal having different spreading sequences on a common carrier frequency is referred to as code division multiple access (CDMA).
- DS-SS provides significant rejection of narrowband interference”.

Also Misra & Enge (2012:373) argue that the reason to use spread spectrum is its ability to combat radio frequency interference. Spread spectrum technique has been used in military applications for many years. Such use of noise-like carrier waves and bandwidths much wider than required had originally two motivations: to resist enemy efforts to jam the communication or to hide the fact that communication was even taking place (Burel 2000).

2.1.2 Signal structure Glonass

While GPS is maintained by the US Government, Glonass is operated by the Russian Aerospace Defense Forces and has 24 operational satellites. Figure 2.2 shows the frequency allocations for Glonass, referred as G1 and G2, and GPS (L1 and L2). In addition the modernized G3 and L5 band together with the Galileo bands are illustrated together with possible interference sources.

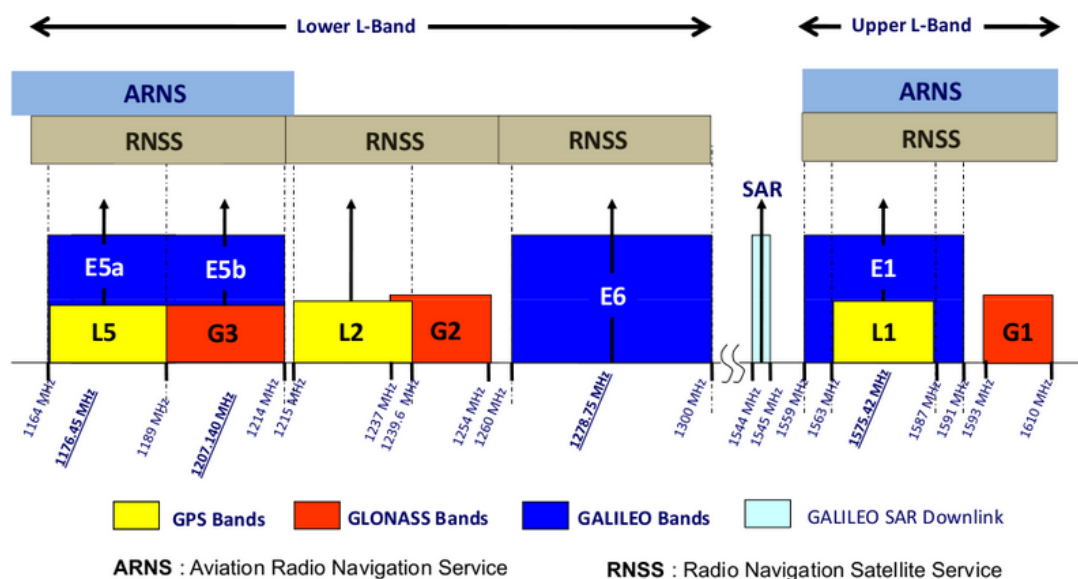


Figure 2.2: GNSS Frequency allocation (Navipedia 2014)

Unlike GPS each Glonass satellite transmits on slightly different carrier frequencies within the G-bands. The high accuracy code is transmitted on both G1 and G2 and the standard accuracy code on G1 (all satellites) and G2 (Glonass-M satellites). The standard accuracy signal has a PRN code consisting of 511 chips which are repeated with a period of 1 ms and a chipping rate of 0.511 Mega chips per second (Mcps). The high accuracy signal has a period of 1 second and a chipping rate of 5.11 Mcps. In comparison to GPS the navigation data message is transmitted at the same rate (50 bps) but the chipping rates of the two Glonass signals are half those of GPS C/A and P(Y)-codes (Misra & Enge 2012).

Glonass satellites transmit the same PRN code at different frequencies using a 14-channel frequency division multiple access (FDMA). The RF carriers are channelized, and at G1 the channel spacing is 0.5625 MHz with 7 channels lower than the center frequency, 1 channel at the center frequency of 1602 MHz and 6 channels higher. The lowest channel has thus center on 1598.06 MHz and the upper most channel has center on 1605.38 Mhz.

These differences in carrier frequencies imply low cross correlations between the FDMA signals, but the negative side is that a receiver needs to synthesize many frequencies. Misra & Enge (2012) speculates on the reason why Glonass chose FDMA instead of CDMA, and suggest it is because a single tone jammer can take out one satellite signal at most in an FDMA system but all signals in a CDMA system.

2.1.3 Signal power

GNSS signals are very weak compared to man-made signals generated on the surface. The radio frequency (RF) power at the antenna input port of a satellite is about 50 watts, and the satellite antenna spreads the RF signal evenly over the surface of earth. The transmitted power is attenuated mainly because of the signal transmission path loss, and it decays with the distance squared when it travel from its orbit to the user (Misra & Enge 2012).

The specifications for the GPS states that the minimum received power level for the users on the earth should be -158.5 dBW for the C/A-code on L1 and -160 dBW for the P(Y) code on L2 (Global Positioning Systems Wing 2010). This is around 10^{-6} W and is well below the background RF noise level sensed by an antenna on the receiver. For Glonass the normalized minimum power should not be less than -157 dBW on G1 (Misra & Enge 2012).

Misra & Enge (2012) and Last (2010) argue that the extremely low signal power that reach the receiver is the Achilles` heel of GPS and support Volpe (2001) by highlighting the concern about the vulnerabilities of the weak powered signals as we rely more and more on GPS.

2.2 Influences on GNSS measurements

The computed range between the satellite and receiver contains biases and errors. The pseudorange is corrupted by receiver and satellite clock offset and atmospheric biases from the ionosphere and troposphere. The ionosphere delay the signal caused by charged particles and radiation from the sun and in the troposphere the variations in atmospheric pressure, temperature, partial water vapor and weather events have effect on the signal. The effects from the troposphere can to some extent be modelled and corrected. Use of two or more carrier frequencies will minimize the ionospheric effect on the range (Bingley 2013).

When the receivers receive reflected signals from surfaces near the antenna multipath occur. Since the path travelled by a reflection is longer than the direct path, observed pseudorange will be too long. If an object obstructs the satellite signal on its path to the GNSS receiver shadowing effects will occur.

The range is also influenced by the geometric distribution of the satellite constellation at the time of measurement. This geometry is measured by the DOP (dilution of precision) parameters. A high accuracy is represented by a low DOP value where there is an even overall dispersion of the satellites while low accuracy with a high DOP value can occur when there is a cluster of satellites in one segment of the sky (Kaplan & Hegarty 2006). For mariners who navigate at sea level the value of Horizontal DOP (HDOP) is important to be aware of.

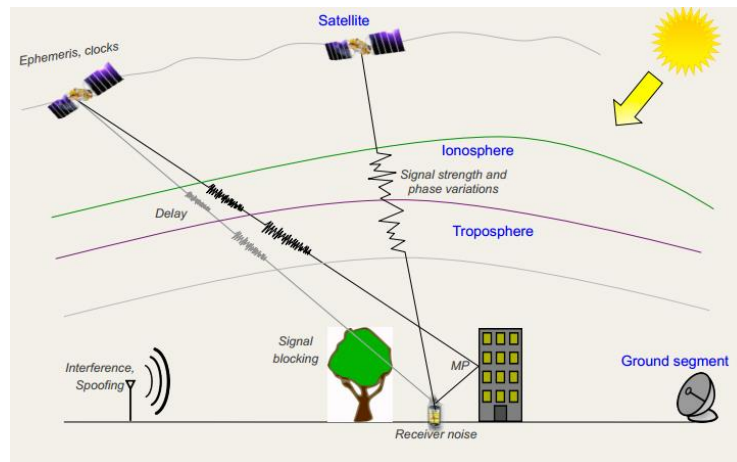


Figure 2.3: Factors impacting GNSS performance (Norwegian Space Center 2013)

All these influences shown on Figure 2.3 have impact on the reliability of civilian type GNSS receivers, and it is important to understand how to mitigate or recognize the presence of them. To use GPS receivers with confidence, knowledge of the influences described above is required (Niekerk & Combrinck 2012). Another serious impact is the susceptibility of civilian GNSS receivers to jamming. When doing an assessment of the vulnerability of the GNSS-system it is of high importance to recognize all these factors which contribute to the performance of GNSS.

2.3 Radio frequency interference

Radio frequency signals from any undesired source that are received by a GNSS receiver are considered as interference. A result of such interference can be degraded navigation accuracy or complete loss of receiver tracking (Kaplan & Hegarty 2006).

Volpe (2001) and Hofmann-Wellenhof (2008) differentiate interference into unintentional and intentional interference. Unintentional interference can come from among others broadcast television, VHF transmitters and personal electronic devices. Findings with regards to unintentional interference in the Volpe-report were that GPS is susceptible to such interference and also ionospheric effects and signal blockage, and the effects were most noticeable to SPS users who use single frequency.

Intentional interference is further categorized into jamming, spoofing (false signal) and meaconing (rebroadcasting). Jamming is defined as “the emission of radio

frequency energy of sufficient power and with the proper characteristics to prevent receivers in the target area from tracking the GPS signal” (Volpe 2001:30).

2.3.1 Characterization of jamming signals

Radio frequency interference (RFI) can be pulsed or continuous. Continuous RFI can be classified by its bandwidth and is usually differentiated into broadband or narrowband (Kaplan & Hegarty 2006:244). This classification is relative to the GNSS band, and implies that a broadband RFI has a bandwidth equal or greater than the GNSS bandwidth (2 MHz for the GPS C/A-code) and a narrowband RFI has a narrower bandwidth. An interference signal consisting of a single tone is called a continuous wave (CW) which is concentrated in a very narrow band around the center frequencies. The CW signal is probably the simplest form of interference.

Moreover, jamming signals can be characterized by its center frequency, whether it is in band or out of band interference, and by its power which is normally expressed as jammer-to-signal power (J/S) in unit of dB.

2.3.2 Classification of jamming devices and their signal characteristics

Mitch et al. (2011) have tested 18 of the current commercially available handheld civilian GNSS jammers with regards to signal properties, and they were grouped into three categories based on power source and antenna type. This categorization is also adopted by Kraus et al. (2011):

1. Jammers designed to plug into a 12 Volt car cigarette lighter socket. These jammers usually have low transmitting power (below 100mW) and possibility to connect an external antenna.
2. Jammers powered by battery and equipped by an external antenna connected via an SMA connector. Some of the jammers are able to transmit on both the L1 and L2 frequency bands, and the transmit power is up to 1W.
3. Jammers disguised as a harmless electronic device, f.ex. cell phones. They have no external antenna and these jammers normally use sawtooth frequency modulation.

All of these jammers broadcasted power at or near the L1 carrier frequency and six of them broadcasted power at the L2 carrier frequency.

Figure 2.4 shows the result of the analysis of a typical jammer from Mitch’s Group 1. On the upper graph, frequency vs. time is plotted and the lower graph shows power vs. time. The upper graph shows a series of linear chirps. Each sweep is on 9 microseconds and covers a range of about 14MHz which include the civilian L1 band. The center frequency is the red horizontal line where the power was measured to 22mW.

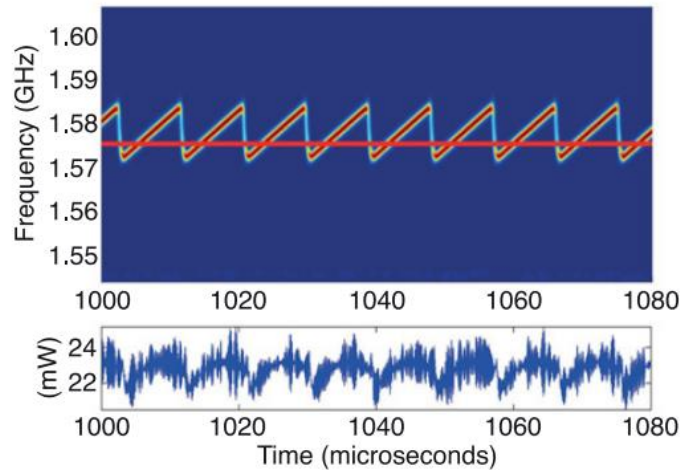


Figure 2.4: Signal characteristics for a group 1 jammer (Mitch et al. 2011).

Most of the jammers in this research transmitted signals with bandwidths exceeding the 2 MHz civilian GPS C/A signals, and some of them had bandwidth exceeding the 20 MHz P(Y) signal. The majority of the jamming signals were generated by frequency modulation of a continuous wave (CW) signal with some sort of swept tone method to generate broadband interference and most of the jammers used linear chirp signals.

Handheld GNSS jammers were also tested in a study at the University of Federal Armed Forces in Munich (Kraus et al. 2011). In accordance with Mitch et al. (2011) this test shows that most jamming devices generate broadband interference. In this case two of the devices transmitted a signal at a single frequency close to the center frequency of L1 that varied with the temperature of the device. The bandwidth of these signals was less than 1 kHz and it could be modeled as CW interference. Figure 2.5 shows the spectrum generated by those two receivers (Jammer 1). Such interference is significantly attenuated by the spread spectrum nature of GNSS codes (Pullen & Gao 2012). The broadband interference generated by most of the jammers

is showed in the right graph in Figure 2.5. The bandwidth of the broadband jamming signal on the figure is about 12 MHz with center frequency close to L1. This spectrum is created by rapidly varying the frequency of a CW-like signal, and the frequency in this example changes linearly from about L1-6MHz to L1+6MHz (Pullen & Gao 2012).

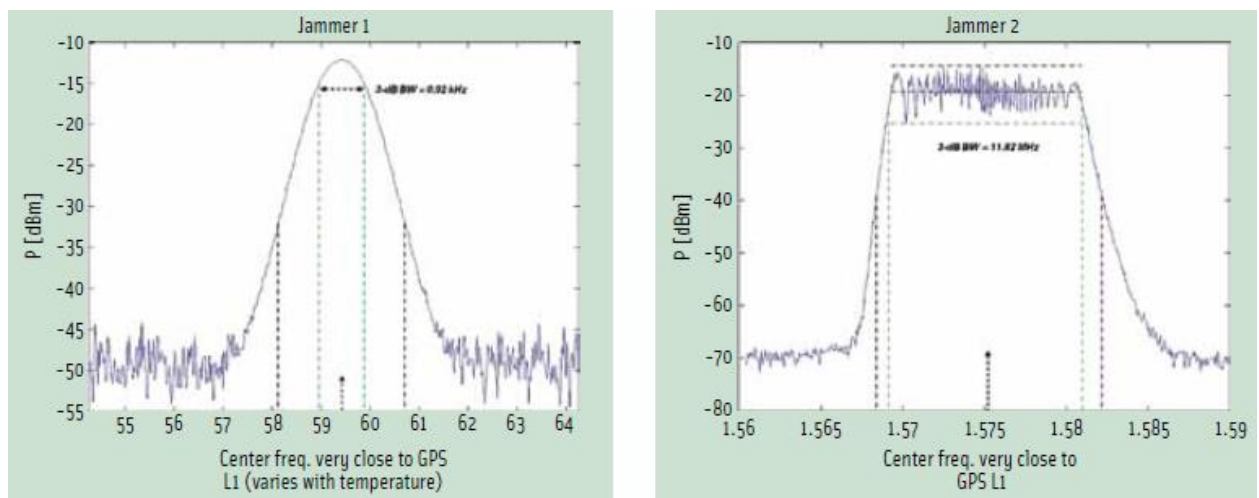


Figure 2.5: Spectrum of CW (1) and broadband jammer (2) (Kraus et al. 2011)

Axell et al. (2013) states with reference to Mitch et al. (2011) and Pullen & Gao (2012) that the current development of GPS jammers with power in the range of 1 to 100 Watt is extensive and even more advanced jammers than those in the three categories as described above is about to appear on the market.

2.3.3 Jamming effects on signal processing

The reason why the receiver can extract the low powered GNSS signal is the knowledge of the signal structure (PRN code). “Processing gain” is the signal boost realized by this mean, and if the noise level is raised by RF interference or jamming there could not be enough available processing gain to extract the signal (Misra & Enge 2012:42). The spread spectrum technique makes it possible to correlate the GNSS signals out from below the background noise.

GNSS is very tolerant of pulsed RFI, even if it is very powerful, because the pulses usually are short in comparison to the duration of a GPS or Glonass data bit, which is 20ms. On the other side GNSS has difficulty to handle continuous RFI whether it is broadband or narrowband or tone interference (Misra & Enge 2012). But the spread spectrum can attenuate narrowband RFI in the correlation process. Figure 2.6 shows

the processing gain of spread spectrum signals against narrowband RFI. The top illustration shows the spectrum of the GPS C/A code and narrowband RFI before correlation with a code replica in the receiver. When the receiver correlates the incoming signals with replica codes the spectrum of the narrowband jammer spreads across the bandwidth as shown in the lower picture and the GPS power is concentrated in a narrowband.

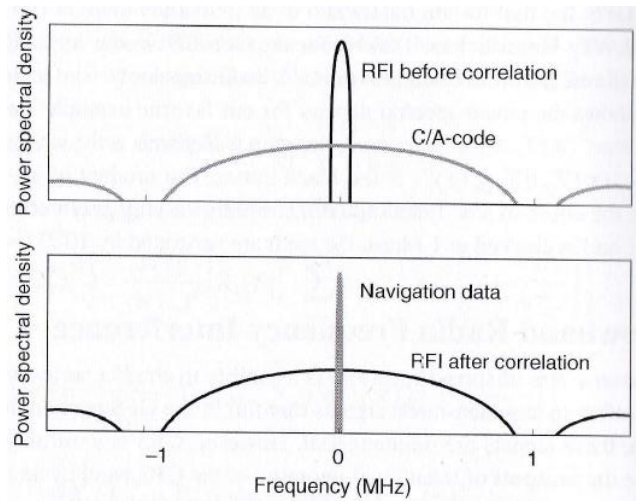


Figure 2.6: Processing gain of spread spectrum vs. narrowband RFI (Misra&Enge 2012)

A calculation made by Misra & Enge (2012:508) figures that GPS can tolerate approximate a tone jammer with 30 dB more power than the C/A signal and 40 dB more power than the P(Y) signal since the P(Y) codes are ten times faster than the C/A code.

If the RFI power is spread across a wider bandwidth, the correlation effect has opposite effect on the GPS signal. When the replica code is aligned with incoming code the receiver will wipe off the incoming code and the GPS spectrum will collapse. The incoming signal is then de-spread and the GPS power is concentrated in a bandwidth of the navigation data which is 50 Hz (Misra & Enge 2012).

2.3.4 Carrier-to-noise ratio

For all receivers jamming will effect in decreased measured signal strength. The carrier-to-noise power density ratio C/N_0 describes the signal strength, and this ratio is a bandwidth-independent index number that relates the carrier power to noise per 1 Hz bandwidth, and is expressed in dB-Hz. According to Hofmann-Wellenhof

(2008) C/N_0 is the fundamental navigation signal quality parameter at the receiver. This is because there is a functional relation between this quantity and the tracking loop. The lowest C/N_0 that the receiver can track is the tracking loop threshold.

The noise is generally described by use of a temperature equivalent parameter, the thermal noise, which is commonly assumed to be white and Gaussian distributed. The noise power density N_0 is defined as (Kaplan & Hegarty 2006):

$$N_0 = k T$$

Where:

$$k = -228.6 \text{ dBW K}^{-1} \text{ (Boltzmann constant)}$$

$$T = \text{Temperature in Kelvin}$$

The noise power density of a typical GNSS receiver is in the order of $N_0 = -201$ to -204 dBW Hz^{-1} . A GNSS signal with a received power at the antenna of 10^{-16} W (-160 dBW) is said to be drowned in noise, and for $N_0 = -204 \text{ dBW Hz}^{-1}$ the carrier-to-noise ratio corresponds to 44 dB-Hz in an unjammed environment.

C/N_0 below 34 dB-Hz is characterized as weak signals (Hofmann-Wellenhof 2008). Rao and colleagues (2013) consider C/N_0 down to 28 dB-Hz for receivers that are stationary or moving with low dynamics for acceptable, and for antennas on platforms with high dynamics C/N_0 threshold levels of between $30\text{-}35 \text{ dB-Hz}$ appears acceptable. The general range of C/N_0 values depends on the receiver used and on the platform dynamics (Rao et al. 2013).

C/N_0 is mainly varying with the elevation of the arriving signal as the signal from high elevation satellites has higher signal strength and is less affected by noise as it reaches the receiver. In presence of jamming the theoretical effective carrier-to-noise density ratio $(C/N_0)_{eff}$ will be as follow:

$$(C/N_0)_{eff} = \frac{1}{\frac{1}{C/N_0} + \frac{J/S}{QR_c}}$$

Where:

- $(C/N_0)_{eff}$ = the effective carrier-to-noise ratio in 1 Hz
 C/N_0 = the unjammed carrier-to-noise density ratio in 1 Hz
 J/S = the jammer-to-signal ratio at the receiver
 R_c = the basic code rate of pseudo random noise (PRN) in chips per second
 Q = the parameters of the spectral distribution of the external radio emission relative to the desired signal spectrum ($Q=2.22$ for a wide-band Gaussian interference (Kaplan & Hegarty 2006))

When the jammer moves towards the receiver, the received jammer power (J) increases relative to the distance (r) according to the free-space loss equation as:

$$J(r) = J_t \left(\frac{c}{4\pi r f} \right)^2$$

Where:

- $J(r)$ = received jammer power in Watt as a function of range
 J_t = transmitted jammer power (W)
 r = range between jammer and receiver (m)
 f = frequency of the jammer (Hz)
 c = speed of light in vacuum (m/s)

The formulas presented above shows that the $(C/N_0)_{eff}$ of a signal will decline as the jamming occurs. At the same time signal acquisition, carrier tracking and data demodulation will deteriorate. When C/N_0 decreases the signals become weaker and when the signal is weak enough the receiver cannot generate ranging measurements anymore and it is not possible to compute a position solution.

Moreover, the equation for $(C/N_0)_{eff}$ shows that a higher PRN code rate theoretically will lead to a lower decrease in C/N_0 under jamming conditions.

A drawback of using the C/N_0 as a measurement of signal quality is that this value will decrease both when the GPS receiver is jammed as a result of increased noise, and when the desired GPS signals is weakened as a result of decreased carrier power (Axell et al. 2013).

2.4 Research on GNSS jamming

The military has for many years been aware of the possibility to jam the GPS signals. SPS can be denied over a great area caused by low powered jammers, and an estimation which was done in 1994 figured that a 1 Watt airborne jammer was able to deny GPS tracking to a receiver that had already got lock-on at a distance of 10 km and that this jammer could prevent acquiring lock at a distance of 85 km (Ward 1994).

2.4.1 Receivers ability to determine position

In recent years there has been carried out additionally research on jamming of civilian GPS signals as low powered jammers have become easily available. A study for the South African National Defense Force was carried out in order to see how easy it is to jam civilian GPS receivers (Niekerk & Combrinck 2012). The susceptibility of four different civilian-type GPS receivers to jamming was tested by using a standard commercial RF signal generator and passive GPS antennas. The signal generator generated a frequency modulation signal on the L1 band at 1575.42 MHz and the signal output strength varied in steps between -3 dBm (0.5 mW) and 17 dBm (50 mW).

The initial test was carried out with a jammer power of 13 dBm (20 mW) and the GPS receivers were moved away from the jammer. This experiment showed that the jammer was able to disrupt all GPS receivers to a distance of approximately 2 km. All the receivers were then placed on the ground level at a distance of 2 km from the jammer, where they could lock on to the available GPS satellites for establishing of a position. The jamming signal generator started on -3dBm and increased until the receivers could not establish a position.

Table 2.1: The ability of GPS receivers to resist jamming (Niekerk & Combrinck 2012)

Signal strength (dBm)	GPS receiver			
	Garmin 60CSx	Garmin eTrex	Trimble ProXH	Topcon GB-1000
-3	P	P	P	P
0	P	P	P	NP
1	P	P	P	NP
4	P	P	P	NP
7	P	P	P	NP
9	P	P	P	NP
10	NP	P	P	NP
12	NP	P	P	NP
13	NP	NP	P	NP
15	NP	NP	P	NP
17	NP	NP	NP	NP

P, indicates the ability to determine a position; NP, indicates that a position could not be determined.

From Table 2.1 we can see that the Trimble receiver had best resistance to jamming. This was attributed to the design of its Zephyr antenna which is able to reject multipath signals and thus the receiver could be less sensitive to low elevation signals transmitted by the jammer at ground level. An observation was also that the Garmin eTrex gain better result than Garmin 60CSX which is a more sophisticated receiver. The most sophisticated receiver, the Topcon, was easiest to jam. There was also a significant difference between receivers on their ability to resist jamming at different signal strengths. The authors concluded that it is easy to disrupt the reception of civilian GPS receivers and that “jamming remains a serious threat to the integrity of navigation that needs further investigation” (Niekerk & Combrinck 2012:4).

A weakness of this study might be that there is no information about the quality of the position when the receivers had the ability to determine it at different jamming signal strengths. It would be interesting to study the performance especially when the jammer strength is close to the threshold before losing track to the satellites.

2.4.2 Jammer-to-signal ratios

Jones (2011) has plotted theoretically values for different CW broadband jammers with power from 10mW to 1kW in Figure 2.7. The limitation of the amount of non-

GNSS interference the receivers can handle when they are still acquiring or tracking the desired signal is the maximum jammer-to-signal ratio (J/S). The J/S decreases with the distance from jammer to receiver. In the same graph the horizontal dashed lines show some typical receiver thresholds.

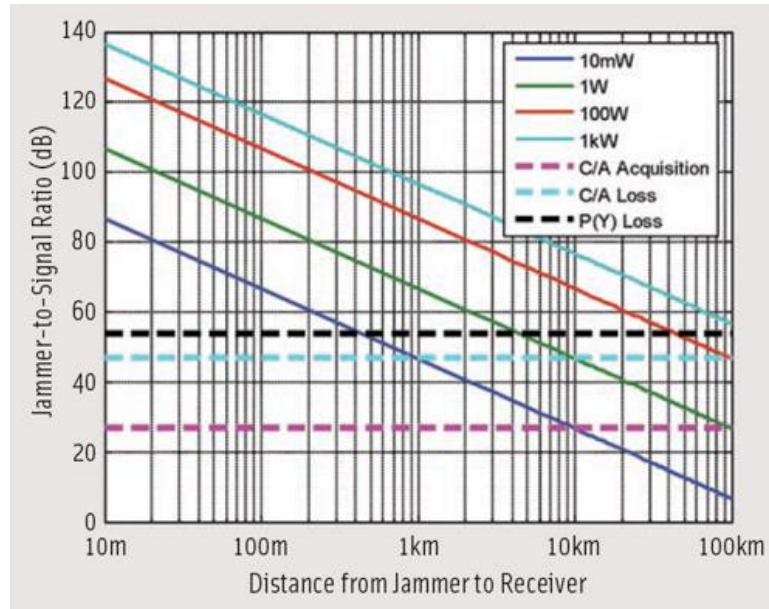


Figure 2.7: The effect of various jammers on GPS receivers (Jones 2011)

As we can see from Figure 2.7, a small 10 mW jammer is able to prevent acquisition to C/A code on distances shorter than 10 km. A receiver that has lock on to the C/A code will in theory lose it when it is nearer the 10mW jammer than 1 km. In comparison a P(Y)-code receiver will lose lock when it is about 300 metres from the same jammer. If a C/A- receiver is exposed to a jammer on 1 Watt it will lose lock on a distance of 10 km. These values are also supported by the findings from Ward (1994) with regards to an airborne jammer.

Another study (Kuusniemi et al. 2012) based on J/S ratios was conducted at the Finnish Geodetic Institute to see how vulnerable consumer grade GPS receivers are. A handheld L1 jammer with an output power of 13dBm that transmitted a chirp signal with center frequency at 1577 MHz and a spectrum bandwidth of 16.3 MHz was used to jam 6 different receivers in a navigation laboratory. The test was conducted with two different J/S ratios (15dB and 25dB). The J/S ratio of 25 dB is close to the theoretical value of the C/A acquisition threshold illustrated by Jones (2011).

When exposed for J/S ratio of 25 dB the best performance receiver provided a position solution all the time with a maximum horizontal error of 22 metres and the worst performance receiver gave position 16% of the time with a maximum horizontal error of 129 metres. The report concluded that the performance results showed significant difference among the receivers, in line with the results from Niekerk & Combrinck (2012).

2.4.3 Carrier-to-noise ratios

Bauernfeind et al. (2011) focused attention on carrier-to noise ratios when conducting an open-field test of jamming signals from typical available low-cost GNSS jammers. This research was done at the Galileo Test Range in Germany, and the results presented here are measured by using a jammer transmitting a chirp signal with a bandwidth of 11.8 MHz in the L1 band. The effective jammer power was -40 dBW (0.1mW), and also this jammer belongs to the category broadband interference.

A multi-frequency Ipex software GNSS receiver was used, and the jammer approached this static receiver starting from a distance of 1200 metres. The carrier-to-noise ratio was measured, and the blue line in Figure 2.8 shows the C/N_0 degradation for this receiver. In addition the red line shows the theoretical curve for effective C/N_0 .

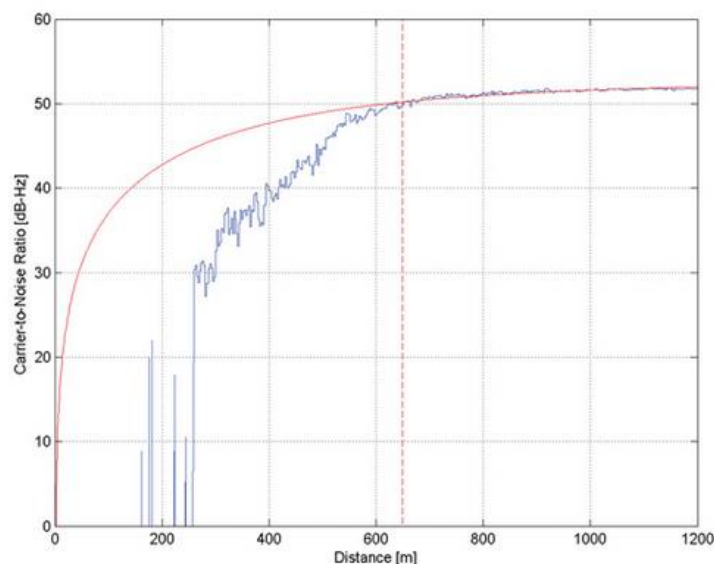


Figure 2.8: C/N_0 for Ipex SW Receiver and the theoretical curve (Bauernfeind et al. 2011)

The authors explain that the measured curves follow the theoretical curves as long as the front end is not saturated. For this interval the received jammer power is

noticeable above the noise floor. Moreover, “when the front-end analogue to digital converter (ADC) is saturated it causes heavily degradation of the signal which exceeds the pure degradation caused by the increased jammer power until loss of lock of signal” (Bauernfeind et al. 2011).

Before the front end was saturated the jammer degraded the correlation process by raising the noise floor, and this degradation caused position errors of more than 50 metres just before the receiver lost track, as shown in Figure 2.9.

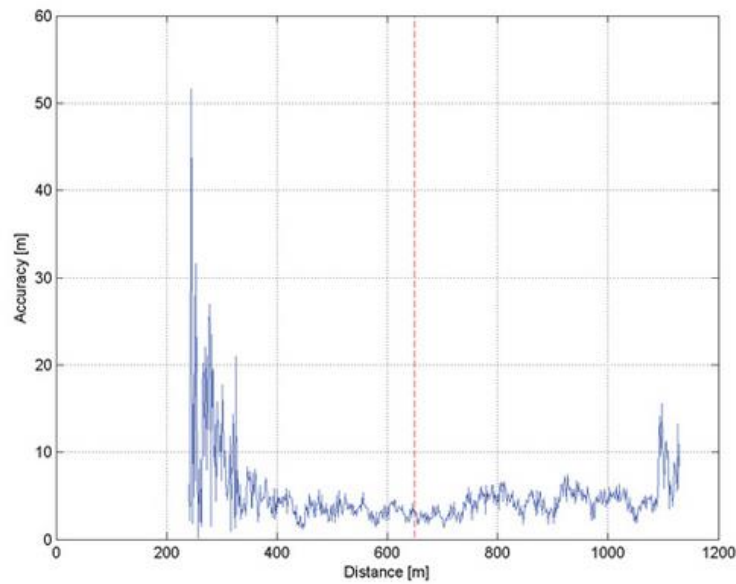


Figure 2.9: Accuracy for Ipex SW Receiver (Bauernfeind et al. 2011)

Also survey grade and mass-market receivers were tested in this experiment, and by comparing them they found that the professional receivers were interfered at a shorter distance but lose lock on the signal earlier. The main conclusion was also here that interference range of a jammer is very dependent on the receiver architecture.

2.4.4 In-band and out-of-band jamming

The research referred to until now have only studied jammer signals inside the GPS L1 band. Another study (Craven et al. 2013) with focus on carrier-to-noise ratios has in addition analysed interference centered outside the L1 band. Craven and colleagues have under laboratory conditions examined the effect of various interference on the tracking capability of a commercially GPS receiver, and the C/N_0 has been measured for the GPS L1 C/A signal to examine the receiver immunity to

interference sources. These interference sources were a continuous waveform (CW) signal and a broadband Additive White Gaussian Noise (AWGN) signal (48MHz bandwidth) both centered on the GPS L1 frequency. The signals from outside the L1 frequency were signals from a GSM centered at 900 MHz, and a DECT (Digital Enhanced Cordless Telecommunications) signal and a LTE (Long Term Evolution) signal both centered at 1900 MHz.

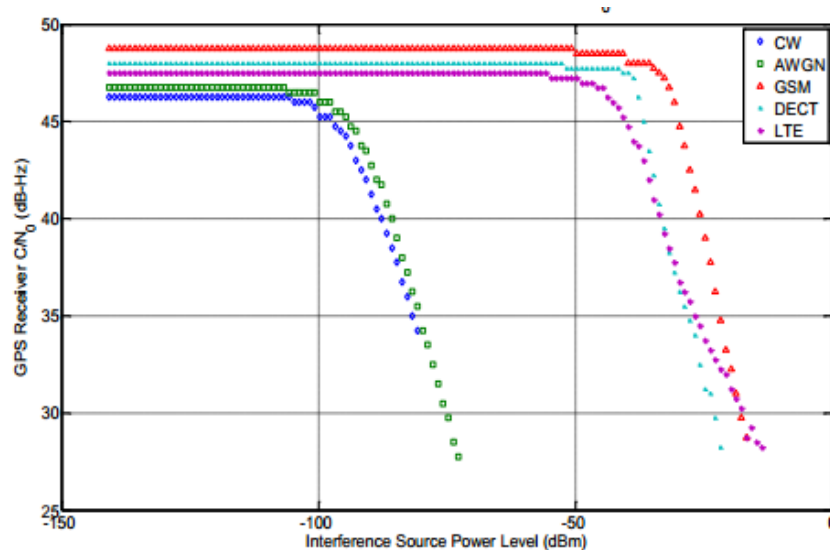


Figure 2.10: C/N_0 as a function of interference power level (Craven et al. 2013)

Figure 2.10 illustrates how the receiver C/N_0 varies as a function of the interference source power level. The result shows that CW and AWGN jamming causes most disruption as these interference sources are defined exactly at the GPS L1 center frequency. In the presence of the CW interference the receiver lost lock at C/N_0 values of 34.4 versus 27.8 for the AWGN broadband noise. The results also show that the interference power of transmissions outside the GPS frequency band needs to be significantly higher to affect the receiver's performance. They further conclude that use of multiple GNSS frequencies will provide jamming immunity because the effect of an intentional interference source which is targeted at a particular GNSS frequency band will likely be less pronounced within an adjacent GNSS frequency band.

2.4.5 Jamming of GPS and Galileo

To supplement this review a research which also has implemented Galileo reception under jamming condition follows. In the absence of available jamming research on

Glomass it is interesting to study how resistant other GNSS systems than GPS are to jamming.

Borio et al. (2013) have investigated the impact of a jammer on GPS and Galileo L1/E1 signal reception. Their experiment was conducted in a GNSS simulator with a survey grade GNSS antenna connected to four commercial GNSS receivers. A cigarette-lighter jammer broadcasting a single saw-tooth chirp signal with a bandwidth of 12MHz was used (Group 1 jammer according to Mitch et al. (2011)). An attenuator was applied to vary the transmitted power and simulate different values of received jammer-to-noise ratio (J/N_0). The relationship between J/N_0 and time was linear starting on a low J/N_0 which was increased to the highest level at the middle of the test time and then decreased.

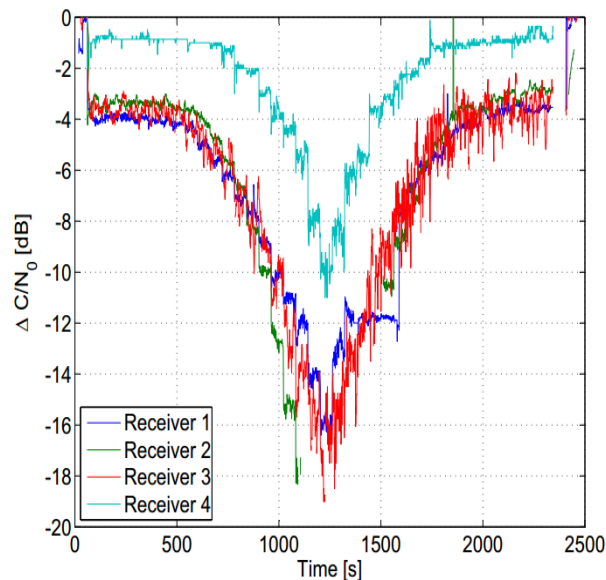


Figure 2.11: C/N_0 loss by four receivers when processing GPS L1 C/A (Borio et al. 2013)

Figure 2.11 shows the average loss in C/N_0 experienced in the presence of the jammer as a function of the J/N_0 for the receivers. Receivers 1-3 are survey grade multi-frequency receivers from three different manufacturers and receiver 4 is a high sensitivity single frequency GPS only receiver. When the jammer was turned on there was a clearly negative jump in the C/N_0 loss curves, and this jump was significantly higher for the survey grade receivers. Borio and colleagues (2013) argue that this is because the HS receiver probably has a front-end bandwidth lower than 12 MHz (the bandwidth of the jammer) and only a small part of the noise caused by the jammer enters the receiver. Unlike the HS receiver, the survey grade

receivers are wideband with front-end bandwidth greater than 12 MHz and therefore experienced a greater initial loss.

Figure 2.12 shows the average C/N_0 loss when processing GPS and Galileo signals in the presence of the jammer in a software-based receiver. Borio and colleagues (2013) state that the GPS and Galileo processing are affected in a similar way but the tracking threshold of the Galileo signals is approximately 6 dB lower than that for the GPS signals. They argue that this is due to the use of a pure PLL processing strategy using only the E1C (pilot) component of the Galileo signal.

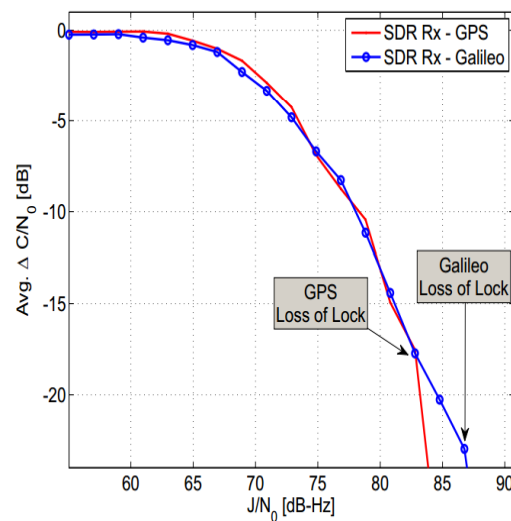


Figure 2.12: Average C/N_0 loss for GPS and Galileo signals (Borio et al. 2013)

Borio and colleagues (2013) argue that since the jammer signal is wideband, GPS and Galileo signals are affected in a similar way. They further claim that receiver front-end has a greater impact in determining the jamming impact than the signal type, and they have shown that narrow band front-ends better shield the receiver against interference. Professional receivers showed a quite similar performance whereas the HS receiver was more resilient to jamming.

2.4.6 Effect of solar radio emission interference on Glonass reception

As there is a gap in research on jamming effects on Glonass, solar radio emission interference, which can be compared to broadband jamming, will be discussed. Vladislav and colleagues (2013) have studied GPS/Glonass performance under strong solar radio emission interference, and their experimental results showed that GPS receivers presented lower noise immunity and that Glonass receivers functions more reliably under conditions with solar emission interference.

In this study, solar radio emission was considered as white Gaussian noise, and the emission intensity was constant within the frequency band of the satellite signal. Further assumptions were that the front-end passband of the GPS receiver radio path was 3 MHz and the passband for each separate Glonass satellite was 0.5 MHz, which are typical receiver values for GPS and Glonass (Kaplan & Hegarty 2006). The solar emission was therefore only considered in these narrow frequency bands.

The result showed that when the solar emission level was increasing the GPS C/A signals carrier-to-noise ratios started to descend earlier and was reduced more noticeably than the Glonass signals. When the solar emission reached a maximum level of 10^6 sfu (solar flux units) the GPS C/N_0 fell below the threshold of minimum allowable C/N_0 at the receiver input while the Glonass C/N_0 still was above this threshold. The fall of GPS C/N_0 at that point was 13 dB whereas the fall for Glonass C/N_0 was 9 dB.

Vladislav and colleagues (2013) explained the better performance of Glonass as a result of the narrower front-end passband of the Glonass receiver for the separate Glonass satellites compared to the GPS receivers. As Glonass uses FDMA technology to separate the signals of each Glonass satellites it requires to set a narrower RF frontend bandwidth compared to GPS. The main expected consequence is lower integral noise power at the analog to digital converter (ADC) input of the navigation receiver. Therefore lower integral power of the solar radio noise will penetrate into a Glonass receiver compared to the GPS, and Glonass can perform its function more reliably under such conditions.

2.5 Maritime GPS and jamming

In order to identify the effects of GPS jamming on safe navigation at sea, the GLA together with the UK Government's Defence Science and Technology Laboratory have conducted a series of two sea trials.

In 2008 a GPS jamming exercise off the coast of Flamborough Head was carried out on the vessel "Pole Star" (Grant et al. 2009). The purpose was among others to investigate the effect from jamming on maritime navigation and safety and to see how mariners cope with a loss of GPS as primary navigation. In this research a jammer with power of 1.5W (2dBW) was used to provide a jamming signal over the

whole 2MHz bandwidth of the civilian GPS L1 frequency. The coverage area of this jammer situated 25 metres above the ground was out to 30 kilometres.

When the vessel entered and exited the jamming region the jamming power was weak, and the two marine grade GPS receivers on board provided position errors up to tens of kilometres away from the true location. The further loss of GPS inside the jamming region caused many alarms on the bridge which all were linked to the failure of different functions to acquire and calculate their GPS position, among others the Automatic Identification System (AIS), the dynamic positioning system, the ship's gyro calibration system and the digital selective calling system (emergency communication system).

Table 2.2: Jamming effects observed on the Pole Star vessel in 2008 (Grant et al. 2010)

State	Ratio of signal strengths	Observed result
1	Jamming signal \ll GPS signals	Normal operation
2	Jamming signal \approx GPS signals	GPS fed equipment provides erroneous data, some of which is hazardously misleading
3	Jamming signal \gg GPS signals	GPS denied and equipment fails to provide any information

The GPS fed equipment was defined to be in one of the three states as defined in Table 2.2. The erroneous GPS positions appeared in state 2. Some of the errors were only a bit different from the true position, which according to Grant et al. (2010) resulted in hazardously misleading information. Further finding during this test was that the main chart and positioning system, the ECDIS, stopped updating because of the GPS failure, which caused a static screen.

The second GPS jamming trial was conducted in 2010 off the coast of Newcastle-Upon-Tyne (Grant et al. 2010). Two scenarios were demonstrated; one with full signal denial where the jamming signal was significantly greater than the GPS signal and another with comparable signals where the jamming signal was slowly increased. The findings on a typical marine grade GPS receiver was that when the jamming signal was comparable with the received GPS signal, data with error was

observed and wandering positions at high speed was reported. When the jamming signal increased the receiver failed to provide any positioning, navigation or timing output. In this case the ECDIS gave an alarm and closed down.

Enhanced Loran (eLoran) was also tested during the second trial, and this system was not surprisingly unaffected by GPS jamming. A closing remark from Grant et al. (2010) was that in the future the combination of GPS, Galileo and eLoran will provide robust and resilient PNT in order to provide safety at sea. They put no emphasize on the fact that there is already another operational GNSS system (Glonass) that used in addition to GPS might provide better performance in a jamming environment.

These two dynamic trials concluded that GPS denial have significantly effects on maritime navigation and safety. GPS is vulnerable, and jamming can cause misleading information and the level of disruption is dependent on the make and model of the equipment installed, the configuration of the equipment and the signal strength of the jamming signal (Grant et al. 2010).

2.6 Conclusion

It is today easy to jam a civilian GNSS receiver, and the receivers react differently when exposed to jamming. Jammers are easily available and they are very effective against civilian receivers on quite large distances. Most of these relatively simple jamming devices generate broadband interference (Mitch et al. 2011; Kraus et al. 2011).

There have been a number of studies where the signal properties of different GNSS jammers have been surveyed and their effect on receivers have been measured by use of GNSS simulators (Borio et al. 2013; Mitch et al. 2011; Kuusniemi et al. 2012). In South Africa and Germany also real outdoor GPS jamming tests have been conducted (Niekerk & Combrinck 2012; Bauernfeind 2011). The findings from these studies are generally that the combination of high sensitivity GPS receivers and the low signal strength from the satellites make GPS receivers vulnerable to jamming.

There is however limited research where both GPS and Glonass signals have been tested with regards to jamming, and where the performance of combined GPS + Glonass receivers have been assessed. This study therefore aims to fill this research gap.

Previous research have shown that it make sense to study C/N_0 under jamming conditions as this is an important quality indicator. The studies referred to which focused on C/N_0 discussed that ratio when the receiver was in tracking phase. Since code acquisition requires a higher C/N_0 than for tracking it will also be of interest to study C/N_0 during the acquisition under jamming conditions.

Moreover, studies have showed that jamming of a maritime GPS has dramatically effects on maritime navigation and safety as many systems on board a vessel depend on the single GPS receiver (Grant et al. 2009; Grant et al. 2010). Grant and colleagues (2010) claimed that eLoran is the solution for resilient PNT. To set up this system a lot of infrastructure is required, and until that is built there might be some advantages of utilizing systems that are already operational. Therefore it would be of interest to investigate how jamming affects the Glonass signals, and assess whether there are any benefits of using Glonass in combination with GPS when it comes to robustness and reliability.

Moreover, Grant et al. (2010) only discussed the performance of marine grade receivers in the dynamic trials. As most of the research papers referred to in this literature review emphasized the fact that jamming is dependent on which receiver that are used, it would also be interesting to test handheld consumer grade and survey grade receivers exposed to jamming in a marine environment in order to make a comparison to a typical marine grade receiver.

3 Methodology

This jamming test is divided into two parts; a static test and a dynamic test. The both parts of the test were conducted in an area north of the Polar Circle in the northern part of Norway (68°57'N - 016°45'E). Permission to conduct jamming in this area was given by the Norwegian Post and Telecommunication Authority under restrictions that the test had to be aborted if there were other vessels closer than 3 kilometres to the jammer source or if fog, heavy snow or rain shower made the visibility poor. The Norwegian National Headquarter for the Armed Forces also had to be informed during all stages of the test.

3.1 Methodology part 1: Jamming of static receivers

3.1.1 Scope

The scope of the first part is to analyse the carrier-to-noise ratios of GPS L1 frequency signals and Glonass G1 frequency signals received by a survey grade receiver when exposed to a jammer. The effects of interference are studied with focus on the carrier-to-noise ratios as an indicator of the quality of the received GPS and Glonass signals from each available satellite. This makes it possible to estimate GPS and Glonass noise immunity. The performance of static standalone survey grade and consumer grade GNSS receivers used in combined GPS + Glonass mode versus pure GPS mode will be assessed with regards to error in the pseudorange position solution, and the effective range in which a low-powered handheld jammer has effect on these receivers will be measured. Measurements of interference influence on GNSS signal acquisition and tracking in a real outdoor environment when the jamming source is applied on different distances are conducted.

3.1.2 Equipment

A Leica GS10 geodetic dual frequency receiver and a handheld consumer grade high sensitivity Garmin etrex 20 receiver were used. Both of the receivers are able to provide a position solution using a combined GPS + Glonass mode in addition to GPS only mode. The Garmin receiver has an integrated antenna, and the Leica GS10 receiver was connected to a Leica AS10 antenna (see Appendix A for further specifications).



Figure 3.1: Leica GS10 receiver and Leica AS10 antenna



Figure 3.2: Garmin etrex 20 receiver



Figure 3.3: L1 frequency jammer (SkyDec)

As previously discussed most illegal jammers are centered on the GPS L1 frequency. Therefore a jammer which broadcasted radio frequency interference centered at the L1 carrier frequency was chosen. Figure 3.3 shows the handheld GNSS jamming device delivered by SkyDec which was applied for this test. The centre frequency of the jammer is 1575.42 MHz and the bandwidth is 60MHz F0. The jammer then covers the frequencies 1545.42 – 1605.42 MHz, and all the 14 Glonass channels on G1 are also covered in the very upper part of the frequency band of the jammer. The

jammer is thus categorized as a broadband jammer, and the average jamming power of this device was measured to 0.33mW (-35 dBW). The jamming power was constant during the trial. To vary the interference strength at the antenna of the GNSS receivers, the jammer approached and was removed from the receivers by use of a small boat.

3.1.3 Test setup

The Leica and Garmin receivers were set up on land in position D marked with a red circle in Figure 3.4. This position is about 3 metres above sea level in an open sky environment. In addition a Leica GS10 base station was set up approximate 60 metres further south in the blue circle (E) (Figure 3.4). Both Leica receivers were set to record GNSS raw data every second and the Garmin receiver was set in combined GPS + Glonass mode for the first part of the test and GPS only mode for the last part logging data every second. Information about number of tracked satellites, their numbers and carrier-to-noise ratios (C/N_0) of received signals from each satellite at the Leica GS10 receivers were recorded in Rinex files.



Figure 3.4: Map of the Site

3.1.4 Procedure

The jammer was applied on a small boat and was mounted about 2 metres above sea level. The test was repeated four times, and the first trial started with turning on the jammer in position A, 2200 metres east of the GNSS receivers. The boat then approached on the yellow line towards the GNSS receivers in point D with constant speed of approximate 7 m/s and stopped in point C, 50 metres from the receivers.

The boat stayed in that position for some seconds before returning back to point B, which was in a distance of 1300 metres from the receivers. At point B the jammer was turned off.

The next three trials started with turning on the jammer at point B, and the jammer approached point C on the same line before returning to point B again. Each time the boat reached point B the jammer was turned off before next trial started. Figure 3.5 is a photo taken at point D and it shows the small boat that approaches the Leica antenna and Garmin receiver.

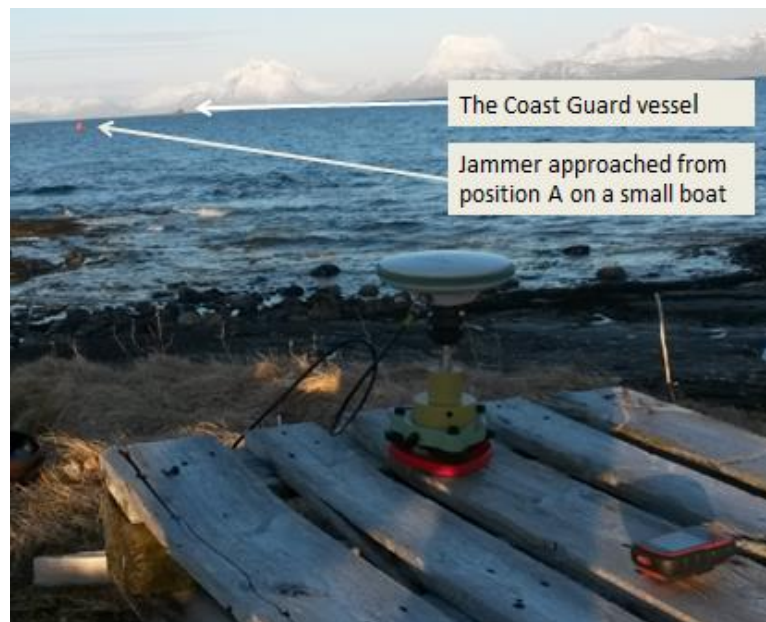


Figure 3.5: Photo taken from the position of the receivers (point D)

3.1.5 Data-analysis techniques

The Rinex data from the two GS10 receivers were post processed in Leica Geo Office using double-differencing to get an accurate position of point D in the red circle. Further code measurements were applied to give the position solution of GPS only and combined GPS + Glonass from the Leica receiver. The Garmin receiver provides 3D position data in GPX-format only, and the precision of the Garmin position solution and the two Leica position solutions were then plotted as a time series to make comparison.

The C/N_0 values for the GPS and Glonass satellites were extracted from the Leica Rinex data using the software TEQC and Matlab, and were further plotted as a time series. C/N_0 values stated in the Rinex files are that for the code solution, and only code solutions will be analysed in this research. HDOP values were extracted from the Leica NMEA data.

3.1.6 Presentation of results

Firstly, the carrier-to-noise ratios to selected GPS and Glonass satellites are plotted for all the four trials in the same diagram together with the distance to the jammer to make comparison of GPS and Glonass signals. Further, Trial 1 is studied in detail by looking at how the carrier-to-noise ratios relate to the horizontal and height precision. Precision is here defined as actual measured position minus the average unjammed position, and the absolute values are calculated.

Calculation of precision rather than accuracy is applied for all the measurements. The horizontal accuracy of the unjammed Garmin receiver was about 4-6 metres compared to the accurate position in point D, obtained by applying double differencing, and the precision for the unjammed periods of the trial was about 0 - 0.5 metres. Since the measurements of the Garmin precision and Leica precision were close to each other, it gives a better overview to compare the precision during the unjammed and jammed stages of the test.

For the Leica and Garmin receivers the precision are plotted for the GPS code solution and combined GPS + Glonass code solution. At last the average fall in C/N_0 for GPS and Glonass satellites during the first jamming trial will be plotted and compared to findings from the simulator test conducted by Borio and colleagues (2013).

3.1.7 Research design issues and limitations

This method is chosen because it allows us to assess jamming in both tracking phase and acquisition phase. Jamming in tracking phase means that the interference signal is turned on after the receiver has performed signal acquisition (i.e. identification of SV numbers and carrier/code synchronization). When turning on the jammer at a long distance from the receivers (point A and B) and then approach them one can assess the receivers' ability of tracking satellite signals when the power of the jamming signal is increasing.

Jamming in acquisition phase means that interference signal is present before satellite signal may be received. While increasing the distance between GNSS receivers and jammer after the receivers have lost the lock, the power of jamming signal will decrease and it make it possible to assess the receivers' ability to acquire useful signal in presence of a decreasing interference source.

Earlier jamming researches have mainly applied a signal generator or attenuator to vary the interference power. One exception is the method applied by Bauernfeind and colleagues (2011) who used jammers with constant power mounted on a car that approached the receivers when they jammed in tracking phase. Their method is quite similar to the one that is applied in this study, and their focus was also on measuring carrier-to-noise ratios. The similarities in the methods make it easier to compare and contrast the results.

To estimate the distance to the jammers Bauernfeind et al. (2011) applied an odometer on the car to get a reference trajectory of the jammer. The reference trajectory of the jammer on board the boat in this study is quite inaccurate and this might be considered a weakness. When the jammer was turned on, also the navigation system on board the small boat was jammed, and the start and stop position of this boat had to be measured by use of the radar on board the Coast Guard Vessel. Because the speed of the boat was constant, the distance to the jammer could be calculated, but the errors of this trajectory are estimated to be up to 20%. Therefore the time is used as reference on the x-axis in most of the plots and the distance to jammer is plotted in its own graph.

It is also important to be aware of that the task of combining mixed GNSS observation from GPS and Glonass in a receiver is subject to biases. Differences in coordinate reference frames and time scales as well as inter-channel hardware biases have to be taken into account. Therefore focus is set on measuring C/N_0 to each satellite in both satellite systems since it is possible to extract isolated GPS and Glonass measurements from the Rinex data. However, comparing a pure GPS position solution to a combined GPS + Glonass position solution might give indications of adding the extra Glonass satellites will improve the performance under jamming conditions.

Another weakness of this research is that the Garmin receiver only provides position solution in GPX-format with no information of C/N_0 ratios. Hence, only the precision in position can be compared to the Leica receiver. Moreover, since only one Garmin receiver is used it is not possible to compare a Garmin GPS + Glonass solution to a Garmin GPS solution within the same trial.

3.2 Methodology part 2: Jamming of dynamic receivers

The second part is a dynamic test where all the measurements are conducted on board the Coast Guard Vessel “Farm” (Figure 3.6).



Figure 3.6: The Norwegian Coast Guard Vessel “Farm”

3.2.1 Scope

The main marine grade GPS receiver on board will be examined when it is exposed to interference, and to make an assessment of its performance it will be compared to the performance of the survey grade Leica receiver and the consumer grade Garmin receiver also utilized in the static jamming test. Further, carrier-to-noise ratios to the GPS satellites will be assessed, and the consequences jamming will have on the ECDIS system on board the vessel will be studied with focus on the ability to handle a loss of GPS input.

As the aim of the dynamic test mainly is to assess the vulnerability of the specific GPS and chart system on board a Norwegian Coast Guard Vessel, the focus during this test will be on GPS performance as this is the only GNSS system applied by the Norwegian Navy. Therefore the two additional receivers (Leica and Garmin) brought on board were set to record GPS observations only.

3.2.2 Equipment and test setup



Figure 3.7: Furuno GP90 receiver (www.furuno.com)

The Coast Guard Vessel is equipped with a stand-alone marine grade Furuno GP90 GPS receiver (Figure 3.7). This is a single frequency L1 C/A code receiver with an update rate of 1 second, and the receiver is connected to a marine grade Furuno GPA019-S antenna mounted on board 13 metres above sea level (Figure 3.8) (See Appendix B for further specifications).



Figure 3.8: Furuno GPA019-S antenna

The similar Leica GS10 and Garmin etrex receivers as used in the first test were utilized in this test to make positioning comparison to the Furuno receiver. The Leica and Garmin receiver were set to record GPS only with an update rate of 1 second. The marine grade Furuno receiver and the Leica receiver were connected to the Furuno antenna via a splitter as shown in Figure 3.9. The Garmin receiver was fastened beside the vessel's GPS antenna.



Figure 3.9: The splitter and Leica GS10 receiver

The ECDIS system on board is named TECDIS (Telchart Electronic Chart Display and Information System) and is delivered by Furuno. This system is approved according to the latest IMO (International Maritime Organisation) regulations.

The jammer used in this dynamic test is the same as utilized in the first static test, and it is applied on the small boat 2 metres above the sea level.

3.2.3 Procedure

This test is divided into two trials:

In the first trial the Coast Guard Vessel was drifting very slowly downstream in a north-eastern direction when the jammer approached it from east on a small boat. The jammer was turned on at a distance of 3000 metres to the Coast Guard Vessel and approached with a speed of about 12 m/s until it was at a closest distance of 50 metres.

In the second trial the jammer was stationary on board the small boat and the Coast Guard Vessel steered a course towards the jammer with a speed of about 5 knots (2.5 m/s). The Coast Guard Vessel started at a distance of about 2000 metres to the jammer and continued until all GPS based positioning systems had lost its input.

3.2.4 Data analysis techniques

Data in form of NMEA sentences was recorded from the Furuno receiver. Rinex data was recorded at the Leica receiver, and the code position solution was extracted. GPX position files were recorded at the Garmin receiver. In addition the C/N_0 was extracted from the Leica Rinex file for each available GPS satellite using the same method as for the static test.

3.2.5 Presentation of results

The carrier-to-noise ratios for the GPS satellites obtained by the Leica receiver in Trial 1 will be plotted. Unlike the static test, the Leica receiver is now connected to a marine grade antenna on a dynamic platform. The distance to the jammer will be plotted in the same way as in the static test. Further the number of satellites tracked by the Leica and Furuno receivers which are connected to the same antenna will be compared.

The position provided by the three receivers will be plotted in Google Earth for Trial 1 and 2. During Trial 2 also screenshots of the ECDIS system were taken which will be used to illustrate its performance.

3.2.6 Research design issues and limitations

As discussed in the literature review a result of the first dynamic jamming test conducted by GLA was a static ECDIS screen and in the second test the ECDIS system closed down. Since the ECDIS systems in both the GLA trials performed an inadequate response to the loss of position sensors, this response will especially be investigated on the ECDIS system on board the Coast Guard Vessel. The focus of the dynamic part of the test will therefore be to assess how the ECDIS system on board the Coast Guard Vessel is able to handle a loss of GPS positioning input.

Grant et al. (2010) emphasized that the level of disruption caused by jamming is dependent on the make and model of the equipment installed and the configuration of this equipment. Therefore, when assessing the ECDIS system it is important to be aware that this assessment is valid only for the system with the specific configuration that is applied on board this specific Coast Guard Vessel.

Similar to the static test only the Leica receiver provided carrier-to-noise ratios for all satellites in view, and therefore no comparison between the different receivers with regards to C/N_0 will be provided. Further, in this trial there also might be some errors with regards to the measurements of the distance to the jammer as this measurements has been done by the radar on board the Coast Guard Vessel.

Further, unlike the static test, jamming is now limited to be conducted when the receivers are in tracking phase only.

4 Results and Discussion

The results and discussion chapter is divided into two parts; one for the static jamming test and one for the dynamic jamming test. For each part the results will be presented first followed by a discussion.

4.1 Static Jamming Test

As explained in the methodology chapter, the static jamming test consists of four trials. First carrier-to-noise ratios for GPS and Glonass signals throughout all four trials will be discussed. Then carrier-to-noise ratios for all satellites and horizontal and height precision performance of the receivers during Trial 1 will be studied in detail. Further, the horizontal precision for the next two trials are discussed in order to support the findings from Trial 1. Moreover, a comparison of the results from Trial 1 with the findings to Borio and colleagues (2013) will be provided to see how a simulator test relates to a test in the real world, and at the end there will be an overall discussion of the findings from the static jamming test.

4.1.1 Satellite coverage

At the beginning of the test, before the jammer was turned on, 8 GPS satellites and 8 Glonass satellites were tracked by the Leica receiver. The skyplot in Figure 4.1 shows the coverage of the satellites for one hour duration for the time period the test was conducted. It summarizes the azimuth and elevation values for each satellite, and shows how the satellites move along the sky. Blue letter G denotes GPS satellites and red letter R denotes Glonass satellites, and it is worth to notice the good Glonass coverage at this high latitude due to the Glonass satellites higher orbit inclination compared to GPS satellites. The dark grey area to the east illustrates the approaching direction of the jammer.

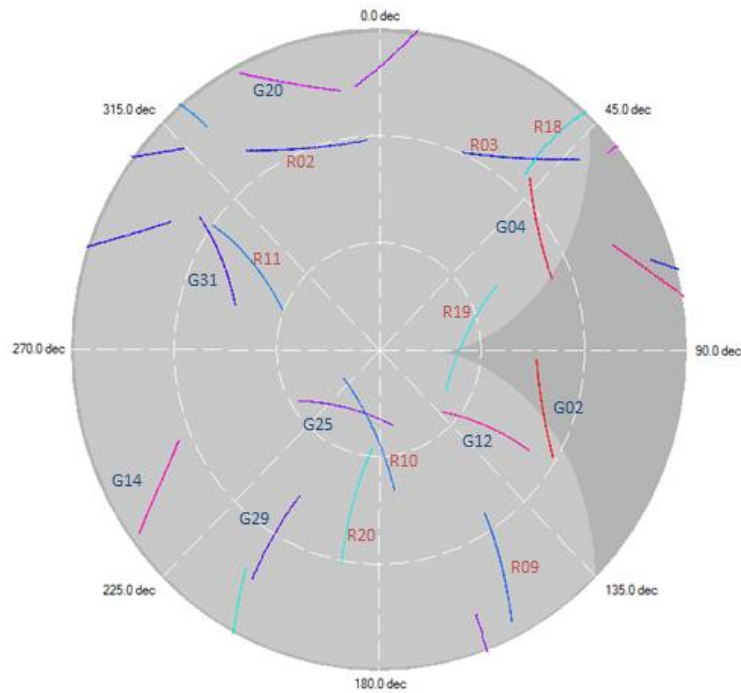


Figure 4.1: Skyplot GPS and Glonass satellites

4.1.2 Carrier-to-noise ratios

This part will discuss the carrier-to-noise ratios obtained during the whole static jamming session that consisted of four trials within 26 minutes. The time representation at the x-axis will be similar for all graphs.

Figure 4.2 shows the C/N_0 values for the whole test period for the two GPS satellites G25 and G02. G02 has an elevation of about 40 degrees while G25 has an elevation of 70 degrees. The black line illustrates the distance between the receiver and the jamming source for the time periods the jammer was turned on. The first trial goes from A to D, the second from E to F, the third from G to H and the last trial starts in I.

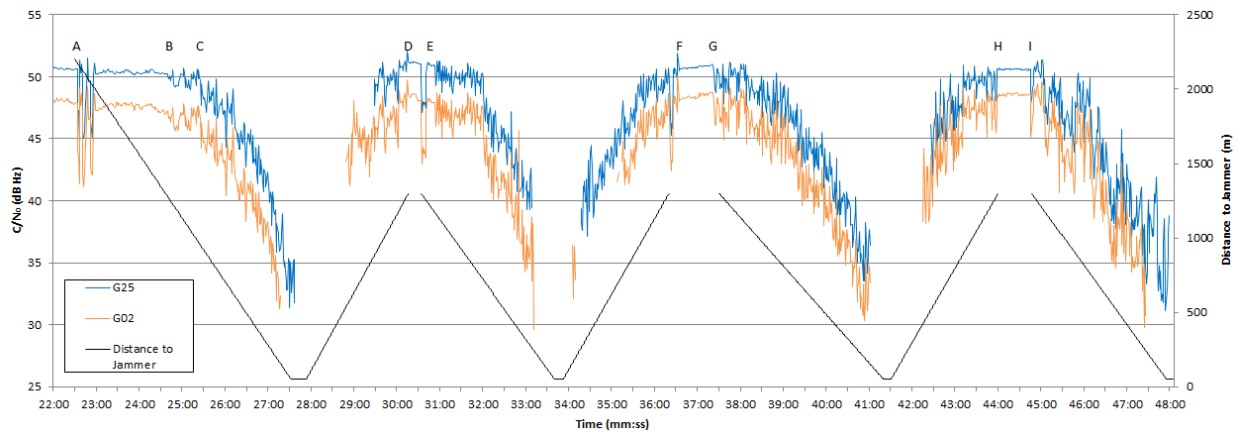


Figure 4.2: C/N_0 for two GPS satellites (G25 and G02) and distance to jammer vs time

From this figure we can see that a low elevation satellite is contaminated with more noise at all stages. Therefore, less effective jammer power is generally needed to lose acquisition for low elevation satellites. Although the two satellites lose acquisition at the same time in trial 2 and 3, we can see in trial 1 and 4 that more interference power is needed before the receiver lost acquisition to the high elevation satellite.

As the jammer was turned on in the first trial at a distance of 2200 metres from the receiver, we can see a clear initial dip in the C/N_0 values from both satellites in point A as they start to oscillate (Figure 4.2). This effect is also shown by Tong (2011) in a simulator test, and similar effects are often seen at the beginning of such an event followed by recovery since the receiver compensates (ibid.). After the initial dip it seems that the receiver is locked onto a stable position for the period A to B as the jammer is approaching. Such C/N_0 dips and oscillating when the jammer is turned on are also evident in the beginning of the next three trials, as shown in point E, G and I (Figure 4.2).

Further, Figure 4.2 shows that some larger fluctuations in the C/N_0 appears when the jammer reaches about 1300 metres (point B), and that the C/N_0 start to drop with approximate the same ratio at a distance of about 950 metres for both the satellites (point C). The receiver lost acquisition to G02 at a distance of 200 metres to the jammer and G25 at 50 metres, both having a C/N_0 of about 31 when losing acquisition. At this trial reacquisition occurred first for G02 when having a C/N_0 of 43 and later for G25 on a C/N_0 value of 47. At point D the jammer was turned off at

a distance of 1300 metres to the receiver and the fluctuations in C/N_0 decreased. The C/N_0 values can be studied in a similar way for the next three trials.

In Figure 4.3 the signals from GPS satellite G25 and Glonass satellite R10 are compared. These are the satellites with highest elevation (65 – 72 degrees) throughout the test and they are close to each other in azimuth in a southern direction as shown in the skyplot.

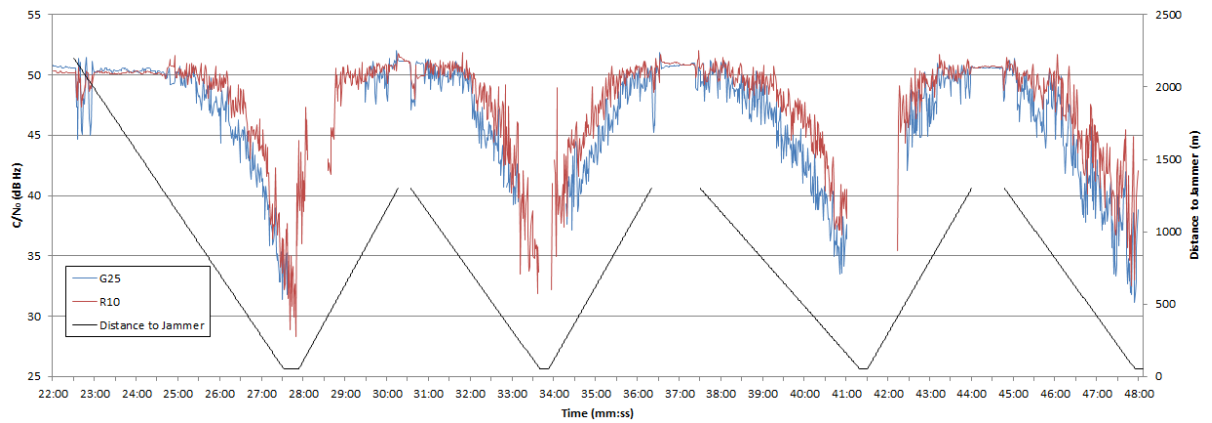


Figure 4.3: C/N_0 for G25 and R10 (high elevation satellites)

In the first trial G25 has approximate 3 degrees higher elevation than R10, and in the last trial 20 minutes later this difference has increased to 13 degrees higher elevation for G25. The two satellites have approximate similar initial C/N_0 values around 50 and also similar C/N_0 values for the periods the jammer is turned off. Figure 4.3 shows that after the initial recovery the C/N_0 values for the satellites start to fluctuate at approximate the same time when the distance to the jammer is about 1300 metres. Further, the C/N_0 to G25 starts to drop at an earlier stage than R10, and acquisition is lost to G25 when keeping a C/N_0 value of 31 while the receiver still is measuring C/N_0 values down to 28 for R10 and continue tracking that satellite when the jammer is on the closest point of approach. Reacquisition for G25 occurred when $C/N_0 = 47$ and for R19 when $C/N_0 = 41$. We can follow a similar pattern with earlier loss of acquisition and later reacquisition for the GPS satellites compared to the Glonass satellites through the next trials in Figure 4.3.

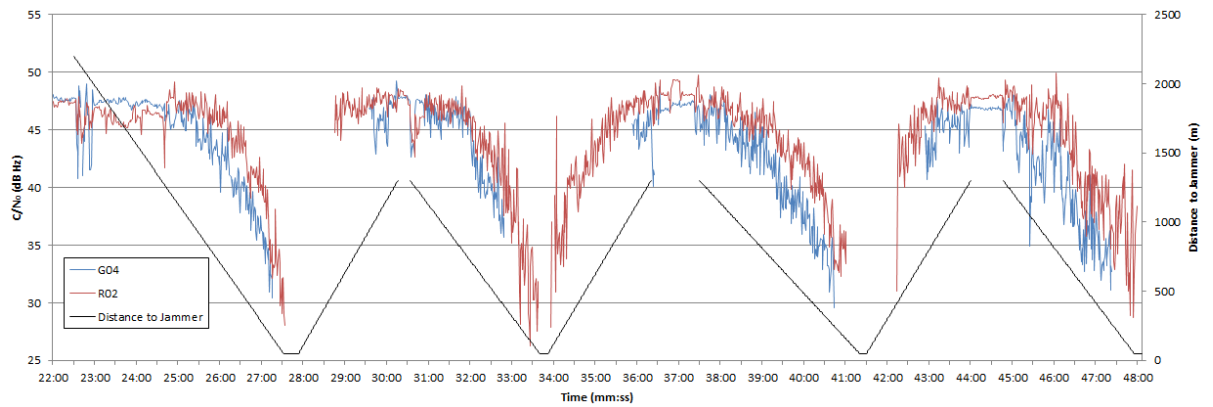


Figure 4.4: C/N₀ for G04 and R02 (low elevation satellites)

Figure 4.4 compares the C/N₀ values to G04 and R02 which both are on a low elevation angle around 30 degrees. They have quite the same initial C/N₀ values of 47, and the satellites are affected in the same way by the jammer as the high elevation satellites (Figure 4.3), with Glonass satellites maintaining signal lock for longer periods of time.

Table 4.1 summarizes the observations of all the GPS and Glonass satellites in view throughout the four trials.

Table 4.1: C/N₀ values for GPS SV and Glonass SV.

	GPS SV		Glonass SV	
	Average	St. dev.	Average	St. dev.
C/N ₀ unjammed	47.3	3.0	45.3	3.7
C/N ₀ when loss of acquisition	32.7	1.8	28.1	2.7
C/N ₀ for reacquisition	42.6	2.6	38.2	2.2

Table 4.1 shows that the values of unjammed C/N₀ have large variation. That is because the satellites have different elevation, and the lower elevation the more noise. When it comes to C/N₀ for loss of acquisition and for reacquisition the variation is a bit lower as these values not are dependent on the elevation of the satellites. In the live jamming research to Bauernfeind et al. (2011) using the IpeX software receiver the average C/N₀ value for the unjammed GPS satellites was about 52, and as Table 4.1 shows the unjammed average C/N₀ value for GPS satellites in this test is about 47. Since Bauernfeind's test is conducted on lower latitudes the

elevation to the satellites are higher which cause higher C/N_0 . The Ipex software GPS receiver lost lock when $C/N_0 = 28$ when exposed to a broadband jammer (bandwidth 11.8 MHz), and the research to Craven et al. (2013) showed that the GPS receiver lost lock at $C/N_0 = 27.8$ when exposed to broadband noise (bandwidth 48 MHz). These values are lower than for the Leica receiver in this test which lost acquisition at $C/N_0 = 32.7$.

The results above indicate that the Leica receiver throughout the jamming test have better ability to keep track on Glonass satellites with lower C/N_0 values than GPS satellites. Moreover, Glonass satellites have a later loss of acquisition and an earlier reacquisition compared to GPS satellites. Figure 4.2 – 4.4 also shows that signals which are received from satellites at low elevation angles are more vulnerable to jamming.

4.1.3 Carrier-to-noise ratios at GPS L2

It is moreover interesting to see that the L1 frequency jammer also has effect on C/N_0 in the GPS L2 band which is within a band 300 MHz lower than the frequency band of the jammer. Figure 4.5 shows that the unjammed C/N_0 on L2 has lower values than L1. This is generally due to the fact that the L2 power at the GPS satellite transmitter output is 6 dB less than on L1 with the C/A code. As the Leica receiver has no access to the military P-code at the L2 frequency it has to use a specific processing technique (semi codeless processing) in order to extract L2 phase and ranging measurements. As a result we get significant correlation losses and the C/N_0 is lowered (Vladislav et al. 2013).

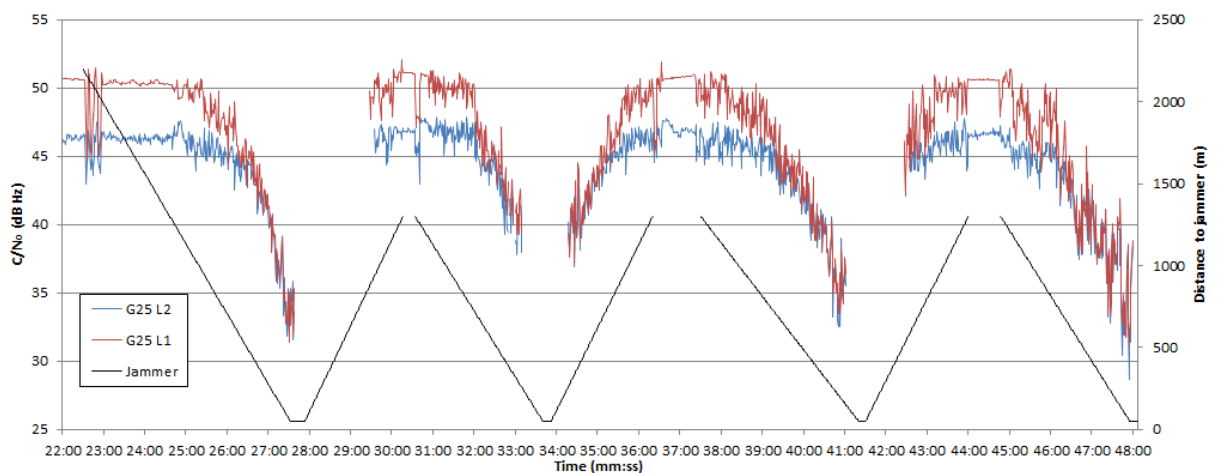


Figure 4.5: C/N_0 for GPS satellite G25 on L1 and L2

During the jamming we can see that the signal on L1 and L2 start to oscillate at the same time. When the jammer power is increasing, C/N_0 on L1 starts to descend earlier, but when C/N_0 on L1 and L2 are on the same level they continue to descend with the same ratio. The oscillation patterns seem to be quite similar, and loss of lock and reacquisition occurs at the same times. The figure shows that the processing of L2 is dependent of the L1 processing, and that a jammer on the L1 frequency also affects the L2 processing for this receiver.

However, studying L2 performance is outside the scope of this thesis, this only give an indication of how dramatically the receiver is affected by the jammer. This specific civilian dual frequency receiver without access to the P-code gives thus no better protection against jamming by using two frequencies since the C/N_0 for the satellites on L1 and L2 are affected in the same way (Figure 4.5).

4.1.4 The first trial

In the following Trial 1 will be discussed in depth. C/N_0 values for all GPS and Glonass satellites tracked are plotted in addition to a plot which shows the average loss in C/N_0 for GPS and Glonass throughout the trial. The total number of GPS and Glonass satellites tracked together with HDOP values is plotted in another graph, and at last the horizontal and height precision to the Leica receiver in GPS mode and combined GPS + Glonass mode are compared to the Garmin receiver in combined GPS + Glonass mode. All these plots for the first trial have the same time representation at the x-axis.

The trial started when the jammer was on a distance of 2200 metres, but there was no significant effect on the C/N_0 values, except from the initial dip when the jammer was turned on, before the jammer reached about 1300 metres. Therefore the largest jammer distances from 2200 to 1550 metres are removed in the following figures. Further we can read from Figure 4.6 and 4.7 that the closest point of the jammer was 50 metres for about 20 seconds, and that the jammer was turned off on a distance of 1300 metres at time 30:16 in the end of Trial 1 when the oscillating of C/N_0 was significantly decreased.

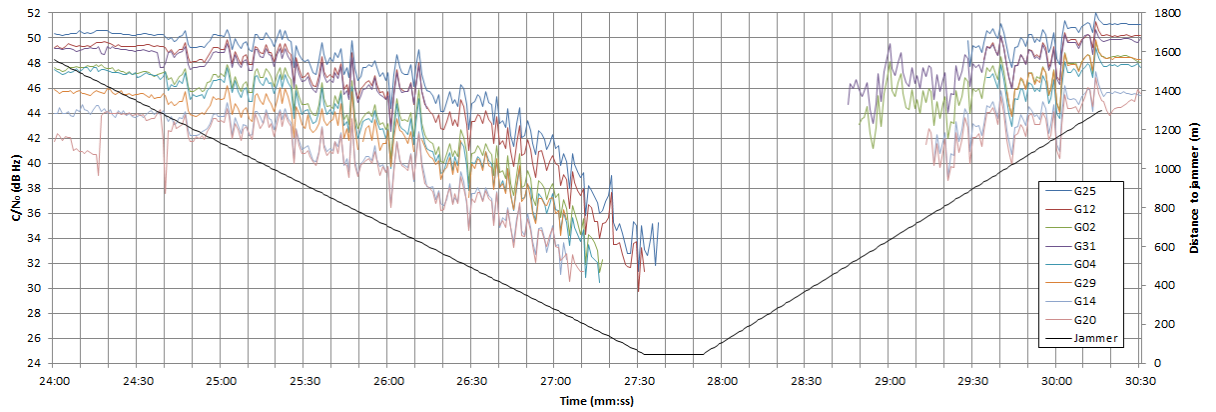


Figure 4.6: Trial 1: C/N_0 GPS satellites

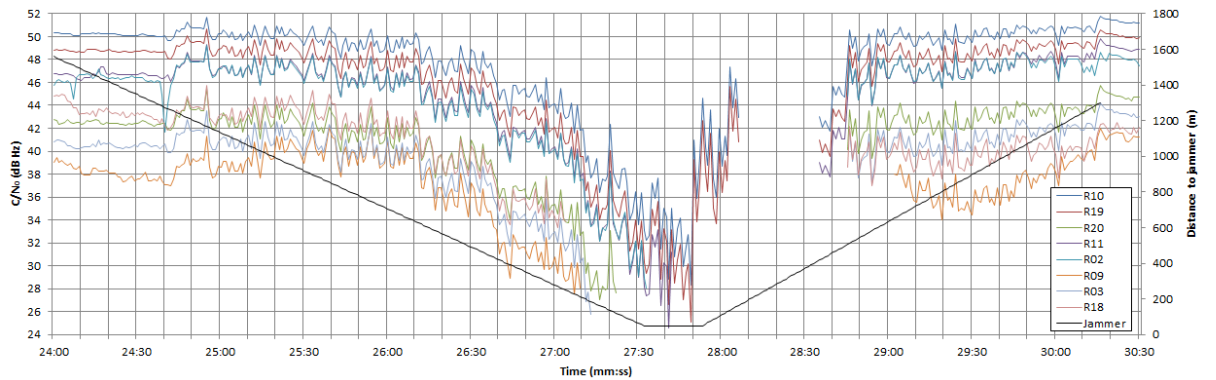


Figure 4.7: Trial 1: C/N_0 Glonass satellites

Figure 4.6 and 4.7 show the C/N_0 for respectively each GPS satellite and each Glonass satellite tracked. At a jammer distance of 1300 metres at time 24:40 we can see that the C/N_0 for GPS and Glonass start to fluctuate at the same time, but the GPS C/N_0 start to descend at an earlier stage when the distance to jammer is about 1000 metres (time 25:25). A significantly fall in Glonass C/N_0 occur later when the distance is about 700 metres (time 26:10). When comparing these two figures we can see that the lowest C/N_0 value for a GPS satellite tracked is 30 versus 25 for Glonass.

Reacquisition for the first GPS satellite occurs at C/N_0 45 versus C/N_0 39 for the first Glonass satellite. We can also see that the two Glonass satellites with highest elevation remain tracked when the jammer is at the closest point of 50 metres to the receiver. The C/N_0 for these two satellites further increase to C/N_0 of about 42 and then the receiver stop tracking them for reasons unknown, but it might be because of certain algorithms within the receiver.

When studying the Skyplot and Figure 4.7 we can also see that the elevation of the Glonass satellites is of greatest significance when it comes to determine C/N_0 . The satellite with the highest elevation (R10) also has the highest C/N_0 , and the C/N_0 descends according to the elevation of satellites until the lowest elevation satellite (R18) with the lowest C/N_0 . One might expect that the Glonass satellites which transmit on the highest frequencies would be less affected by the jammer since they are in the very upper end of the jammer's bandwidth, but the pattern of the higher elevation the higher C/N_0 is consistent during the trial.

Overall, when focusing on all GPS and Glonass satellites in view, the trial reveals that the receiver generally loose track on GPS satellites on an earlier stage and at higher C/N_0 values and also have a later reacquisition at higher C/N_0 values compared to Glonass as shown in Table 4.1.

Further, the average C/N_0 values for the GPS and Glonass satellites tracked are calculated, and Figure 4.8 shows the average loss in C/N_0 relative to the initial values before jamming.

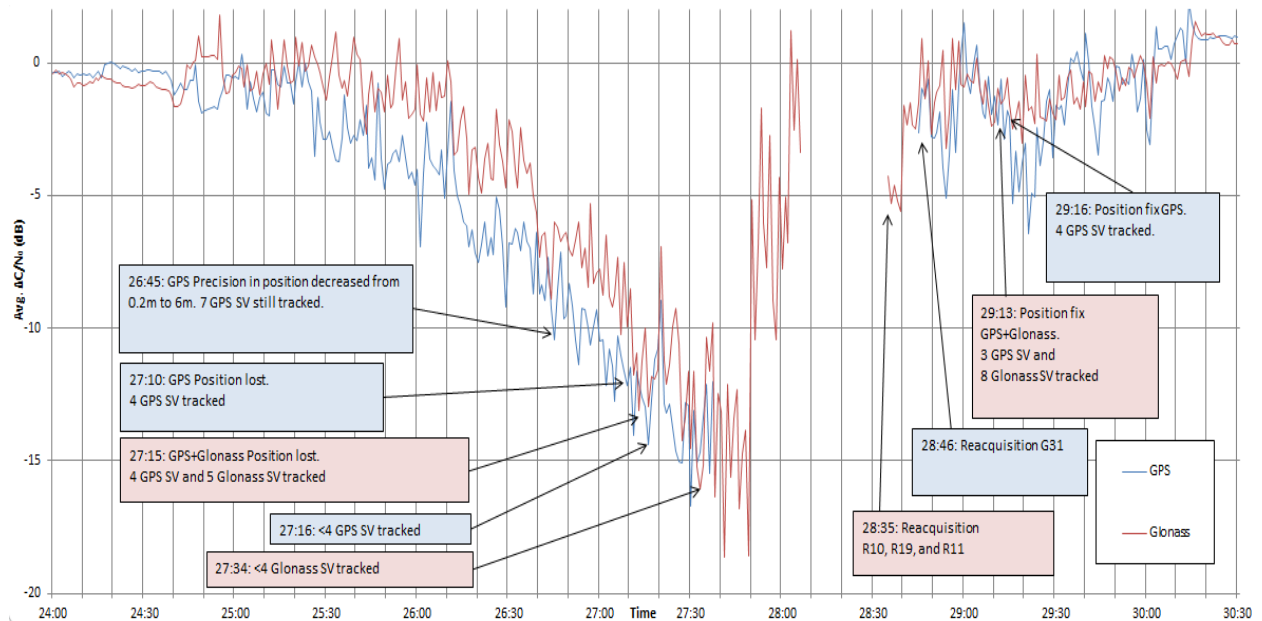


Figure 4.8: Trial 1: Average loss in C/N_0 for GPS and Glonass satellites

When studying Figure 4.8 in relation to Figure 4.9, which shows the horizontal precision for the position solutions, we can see that the first significantly change in precision for the Leica GPS only solution occurred when the average loss in C/N_0 for the GPS satellites was about 10dB (time 26:45). At this time the precision jumped

from around 0.2m to 6m. The precision in the combined GPS + Glonass solution also decreased at that point, but only from 0.2m to 0.6m. The average loss in C/N_0 for Glonass satellites at that point was about 7 dB.

Further, the GPS fix is lost at an average C/N_0 loss of 12dB (time 27:10), when still tracking 4 GPS satellites. At an average C/N_0 loss of 14 dB less than four GPS satellites are tracked (time 27:16). At that point we can see the average C/N_0 loss is decreasing because only the three satellites with highest elevation remain in the calculation of the average values. The combined GPS + Glonass fix is lost 5 seconds after the loss of the GPS only fix, but at this stage still 5 Glonass satellites are tracked. 4 or more Glonass satellites are tracked until the average loss in C/N_0 for the Glonass satellites is 16dB (time 27:34). Still two Glonass satellites are tracked when the average loss in C/N_0 is 18dB and they remain tracked when the jammer is at the closest point as described above.

Reacquisition occurs first for the Glonass satellites when the average C/N_0 loss is 5dB (time 28:35) and on a later stage for the GPS satellites when the C/N_0 loss is about 2.5dB. We can see that the reacquisition time for Glonass satellites is much faster than for the GPS satellites. The first 3 Glonass satellites start tracking again at the same time, and a few seconds later 7 Glonass satellites are tracked when just one GPS satellite is tracked. The position fix occurs first for the combined solution when 3 GPS satellites and 8 Glonass satellites are tracked, and the precision for the combined solution is better at the time of fix than the GPS only solution as shown in Figure 4.9.

A pure Glonass receiver could probably have given position fix on an earlier stage as the algorithm in a combined receiver requires at least one healthy GPS satellite to provide a combined solution because of different time reference in each system.

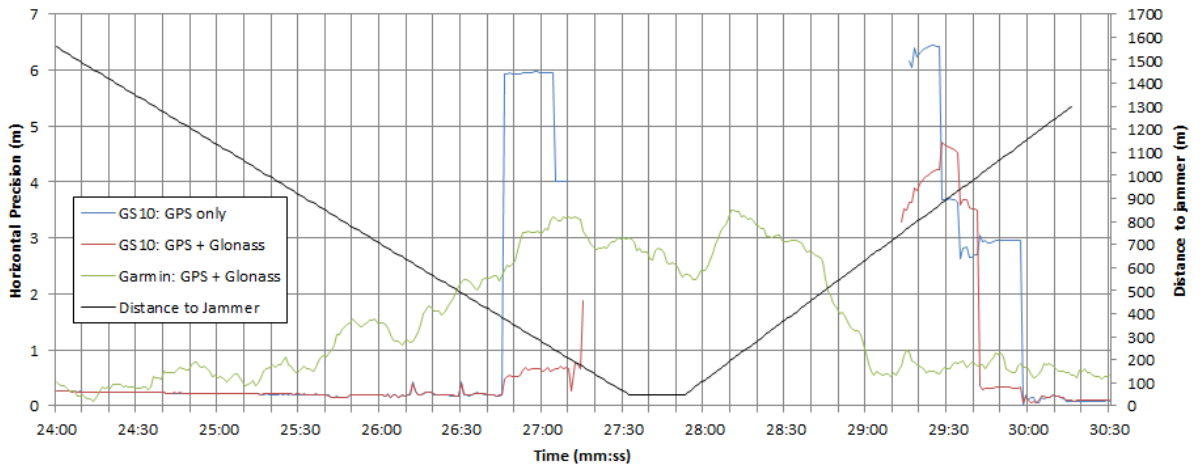


Figure 4.9: Trial 1: Horizontal Precision

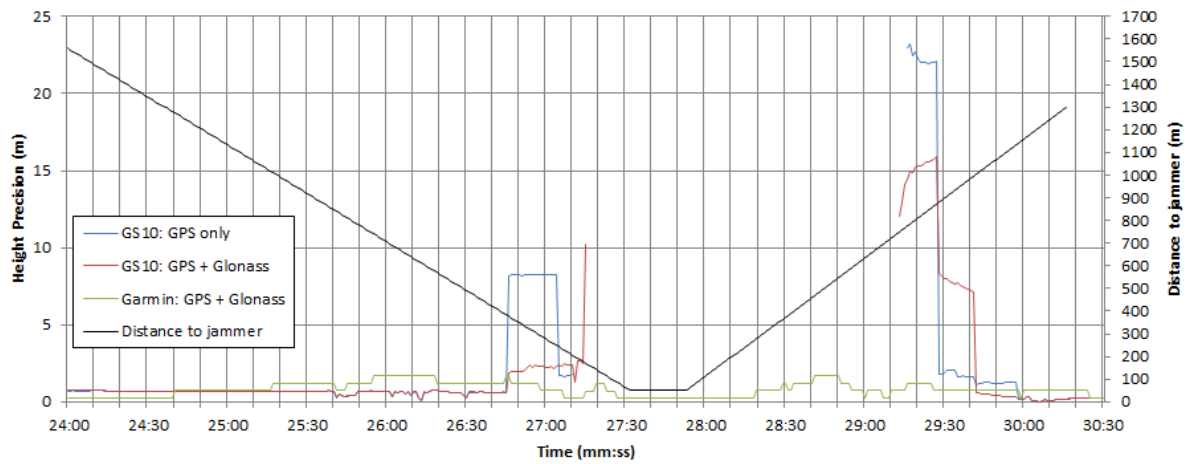


Figure 4.10: Trial 1: Height Precision

Figure 4.9 and 4.10 show the horizontal and height precision for the Leica receiver in GPS only mode and combined GPS + Glonass mode and the handheld Garmin receiver in GPS + Glonass mode respectively. From this trial we can see that a combined GPS + Glonass mode gives better precision than GPS only when the receiver is exposed for the jammer. The gap in position solution is also shortest for the combined mode. We can also see that the Garmin receiver is affected by the jammer at an earlier stage when the interference power is lower, but provides a horizontal position solution which is better than 3.5 metres during the time of the jamming trial when the survey grade receiver gave no position.

As a summary of this part Figure 4.11 gives an overview of number of GPS and Glonass satellites tracked during Trial 1. We can see that the number of GPS satellites drops faster than the number of Glonass satellites when the jammer is approaching. During the reacquisition the number of Glonass satellites tracked grows with a significantly faster rate than number of GPS satellites. This figure shows that the Leica receiver has significantly better ability to track Glonass satellites than GPS satellites when exposed to the jammer.

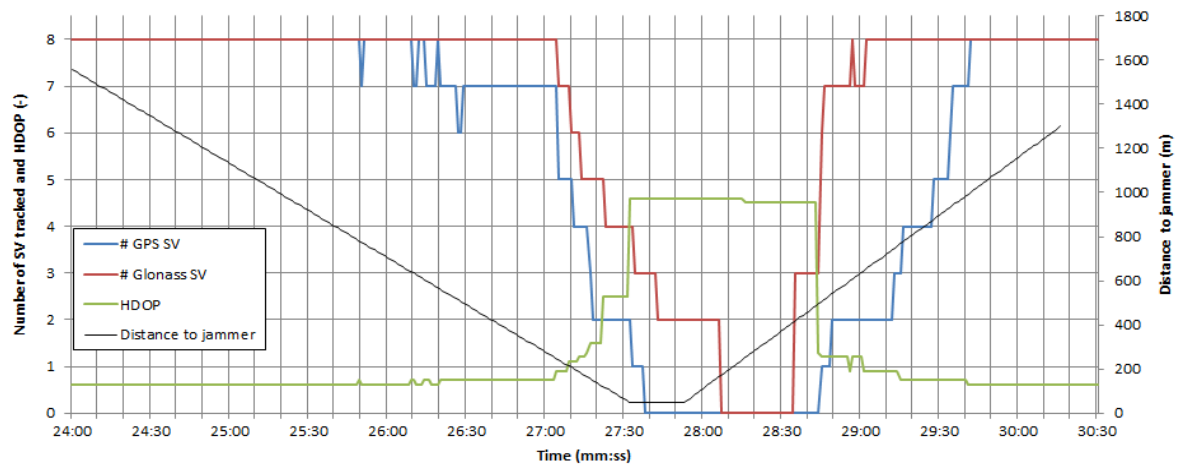


Figure 4.11: Trial 1: Number of GPS and Glonass SV tracked and HDOP

The Horizontal Dilution of Precision (HDOP) is an important quality indicator, especially for the mariner. The interference degrades the performance of the receiver by causing loss of lock on some satellites and the HDOP (taken from NMEA data) increases as the geometry of the remaining satellites become worse as shown in Figure 4.11.

4.1.5 The second and third trial

The findings in the first trial with regards to horizontal precision will in this part be supported by the findings in the next two trials, and they will therefore only be briefly discussed. The difference between the trials is that the Garmin receiver is set in GPS only mode in Trial 3. In the two first trials it was set in combined GPS + Glonass mode.

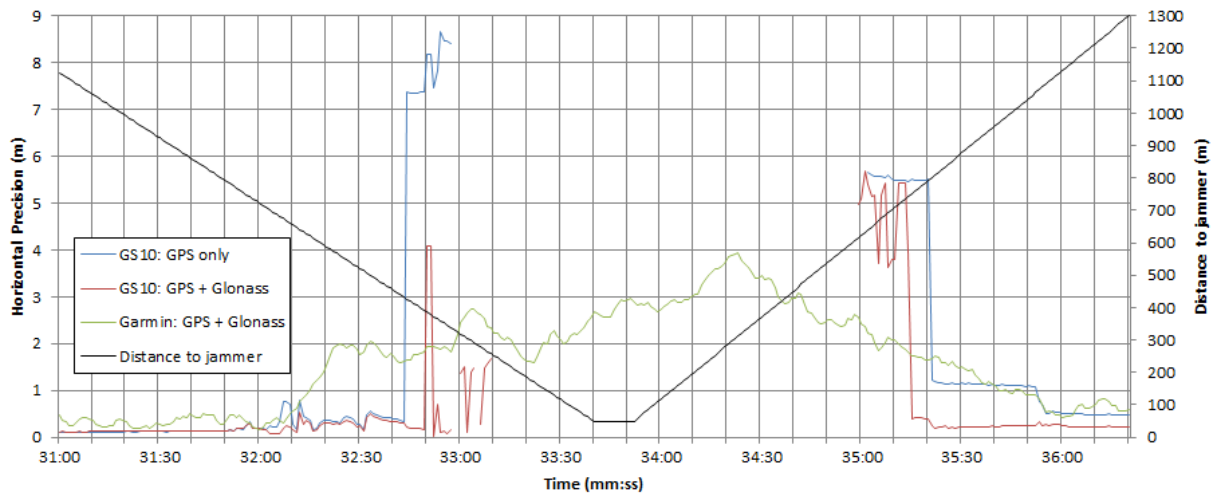


Figure 4.12: Trial 2: Horizontal Precision

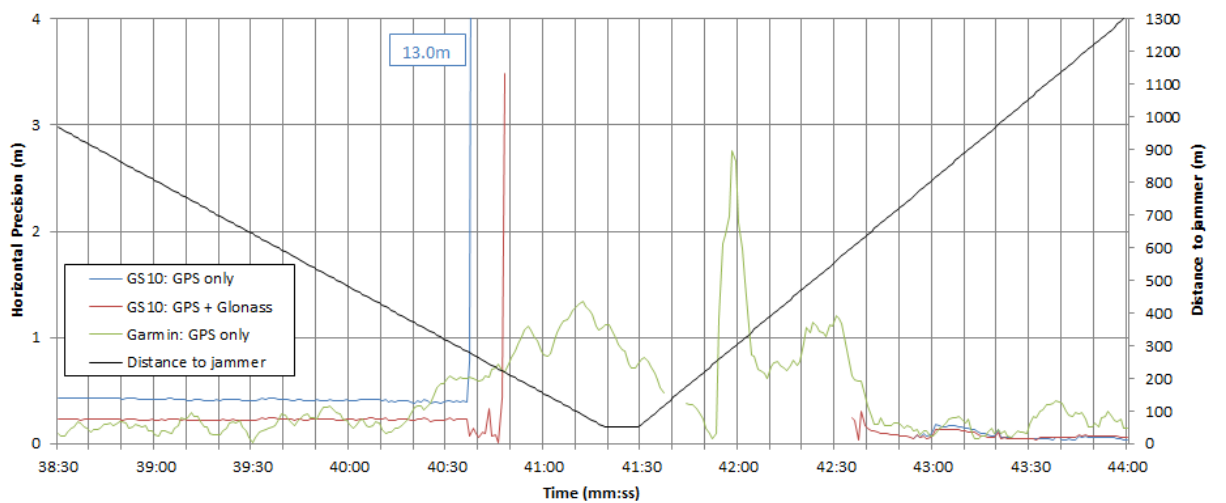


Figure 4.13: Trial 3: Horizontal Precision

The horizontal precision for Trial 2 and 3 are illustrated in Figure 4.12 and 4.13. These two trials also show better precision for the combined GPS + Glonass solution compared to the GPS only solution in the Leica receiver when the jammer has effect. There is also a later loss of position fix and earlier calculation of new position for the combined GPS + Glonass solution.

We can see that the Garmin receiver is affected by the jammer on a longer distance, but it is able to keep on tracking enough satellites to make a position fix for the whole period when using combined GPS + Glonass mode as shown in Figure 4.12. In trial 3 the Garmin receiver was configured to use only GPS satellites, and as Figure 4.13 illustrates there is for the first time a position gap in the Garmin receiver which last for 7 seconds.

For all the trials where the Garmin receiver provided a position fix the precision in horizontal position was better than 4 metres. The worst horizontal precision for the Leica receiver in GPS only mode was about 13 metres (Trial 3) and in GPS + Glonass mode the worst horizontal precision was 5.5 metres in (Trial 2).

Table 4.2 summarizes the findings from the three trials described above with regards to distances to the jammer when the Leica receiver loose position fix and obtains new position fix. The table shows that the receiver in combined GPS + Glonass mode tolerates higher jammer power.

Table 4.2: Distance to jammer when loss of position and obtaining new position fix

	Distance to jammer when loss of position fix (m)		Distance to jammer when obtaining new position fix (m)	
	GPS	GPS + Glonass	GPS	GPS + Glonass
Trial 1	242	171	775	749
Trial 2	339	258	641	615
Trial 3	267	213	766	608
Average	283	214	727	657

4.1.6 Comparison of the first trial versus simulator jamming tests

In this part the findings from Trial 1 will be compared to the findings of Borio and colleagues' (2013) which used a 12 MHz bandwidth jammer in a simulator test.

Figure 2.11 and 2.12 in the literature review illustrate their findings.

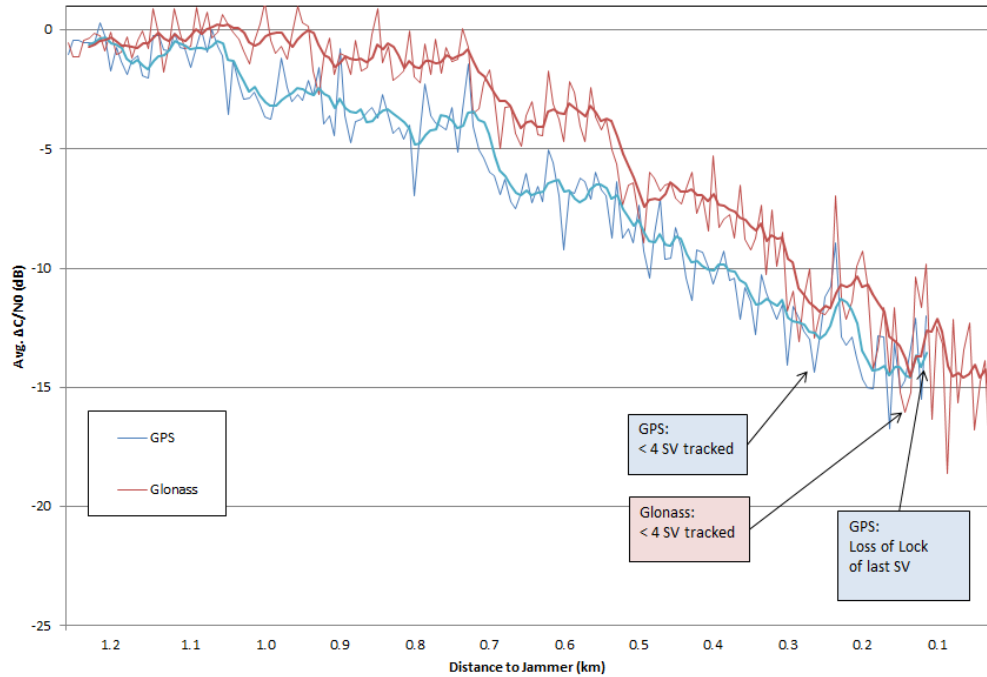


Figure 4.14: Average C/N₀ loss for GPS and Glonass vs distance to jammer

Figure 4.14 shows the average C/N₀ loss for the GPS and Glonass signals for Trial 1 where the fluctuations have been smoothed out in a trendline. The distance to the jammer represents the x-axis.

The figure illustrates that the Leica receiver can tolerate a loss in C/N₀ of about 16 dB for the GPS satellites before losing lock versus about 18dB for the only survey grade receiver that lost lock in Borio and colleagues’ (2013) test (Receiver 2) as shown in Figure 2.11. Their survey grade Receiver 1 and 3 tolerated losses on respectively 16dB and 18dB without losing lock. Also their software receiver in Figure 2.12 lost lock on GPS satellites at an average fall in C/N₀ of 18 dB, and this show that the simulator test by Borio and colleagues (2013) is comparable to the live jamming test conducted in this trial.

As discussed earlier regarding the Glonass satellites, we can see from Figure 4.14 that two of the satellites are still tracked when the loss in C/N₀ is more than 18dB when the jammer power is at the highest level.

4.1.7 Discussion

The static jamming test has shown that as the intensity of interference increased the C/N₀ of both GPS and Glonass signals descend and the pseudorange measurement

precision declined leading to the loss of positioning precision and at last a total loss of lock.

Furthermore, the test has shown that during the acquisition phase the receivers are much more susceptible to interference than in the tracking phase. This applies for both the GPS and Glonass signals, and it is mainly because the bandwidths of the tracking loops have to be higher during acquisition since the Doppler shift is not precisely known (Bauernfeind et al. 2011). When the receiver is in tracking phase the code and carrier tracking loops are already locked on to the signals. Such conditions make jamming harder, since higher power is required to unlock these loops.

As a combined GPS + Glonass receiver has been used in this test it is not possible to give an assessment of the accuracy or precision of the Glonass system compared to GPS under influence of interference. We have however clearly seen that employing Glonass satellites in addition to GPS satellites in the receiver contribute to a later loss of position fix and an earlier calculation of new position. Since the Glonass PRN code is shorter (511 chips vs 1023 chips for GPS) as it use different frequencies to recognise the satellites, the receiver only have to store half as many search hypotheses when looking for a signal. This in turn requires less amount of RAM to conduct an acquisition search, and it takes shorter time to acquire the Glonass signal compared to GPS.

Moreover, the test has shown a significant difference between the GPS and Glonass signal with regards to C/N_0 values. The C/N_0 ratios for Glonass are less affected by the jammer used in this test. As the centre frequency of the jammer was exactly at the GPS centre frequency it might be expected that the jammer would not influence the Glonass satellites in the same way as GPS satellites. The results showed that the Glonass satellites provided better performance as the curve for the average loss in C/N_0 for Glonass was above the curve for GPS at all stages. However, this test showed that the Glonass satellites were able to continue tracking at a higher loss in C/N_0 , and that result is independent of the centre frequency of the jammer.

An implication of the higher chipping rate for the GPS signal is a wider signal bandwidth, which in turn implies a need for wider RF front ends at the receiver compared to Glonass. Also since Glonass utilizes FDMA to separate the signals of

particular Glonass satellites it requires a narrower RF front-end bandwidth, and narrow band receivers are less impacted by the jammer since they are able to filter out a greater portion of the interfering signal.

The results in this test support the findings of Vladislav and colleagues (2013) who studied GPS/Glonass performance under strong solar radio emission interference. Their results showed that GPS receivers presented lower noise immunity and that Glonass receiver can perform its function more reliably under conditions with solar emission interference. They argued that the better performance of Glonass was caused by the narrower front-end passband of the Glonass receiver for the separate Glonass satellites compared to the GPS receivers. This might also be an explanation to the better Glonass performance for our jamming test.

Another aspect is that combined GPS + Glonass receivers can receive signals from more satellites and therefore show more resistance to jamming than a single GPS or Glonass receiver. The test showed clearly that availability and precision benefits of adding Glonass become more significant the more challenging the environment was.

The jamming tests have showed that both the Leica and Garmin receivers have decreased performance in the presence of jamming and that the receivers react differently. Different receiver RF front-end bandwidths may allow different total amounts of jammer power to pass through them. As the Garmin receiver is a narrower-band receiver it is less impacted by jamming because it is able to filter out a greater portion of the interfering signal.

The Leica receiver is interfered at a later point but loose lock on to the signal earlier compared to the Garmin receiver. This is in accordance with results from Bauernfeind et al. (2011) where professional receivers were compared with mass market receivers. Also Niekerk & Combrink (2012) found when testing a Garmin etrex receiver that this receiver had better resistance to jamming than a more sophisticated Garmin receiver as the receiver sensitivity plays an important role here. An interesting point is that the Garmin receiver provided a position solution under jamming condition all the time it was set in GPS + Glonass mode, but provided position gap when it was configured to receive GPS only.

4.2 Dynamic jamming test

The dynamic part consists of two trials. In Trial 1 the Coast Guard Vessel was drifting slowly downstream while the jammer approached it, and in Trial 2 the Coast Guard Vessel steered a course towards the jammer which was static.

The jamming effect on the three different receivers in Trial 1 will be presented first. Then the effect on the receivers in Trial 2 will be studied. Further the effects on the ECDIS system in Trial 2 will be briefly analysed, and at the end there will be a discussion to sum up the findings from this part.

4.2.1 Trial 1: Jamming effects on the GPS receivers

Figure 4.15 shows the GPS skyplot for the one hour period the dynamic test was conducted, and it shows especially that there are no GPS satellites with high elevation to the north as the measurements are conducted at high latitudes. Also in this trial the jammer approached from the eastern direction as illustrated in the skyplot.

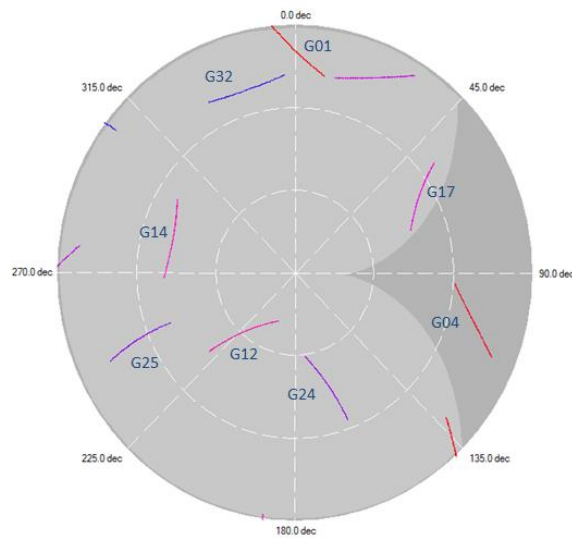


Figure 4.15: Skyplot GPS satellites

Figure 4.16 shows the C/N_0 values for all the GPS satellites tracked in trial 1, and the figure and skyplot show that the four satellites with the highest elevation (G24, G17, G14 and G12) have the highest unjammed C/N_0 , and these satellites are also tracked for the longest time when exposed to the jammer.

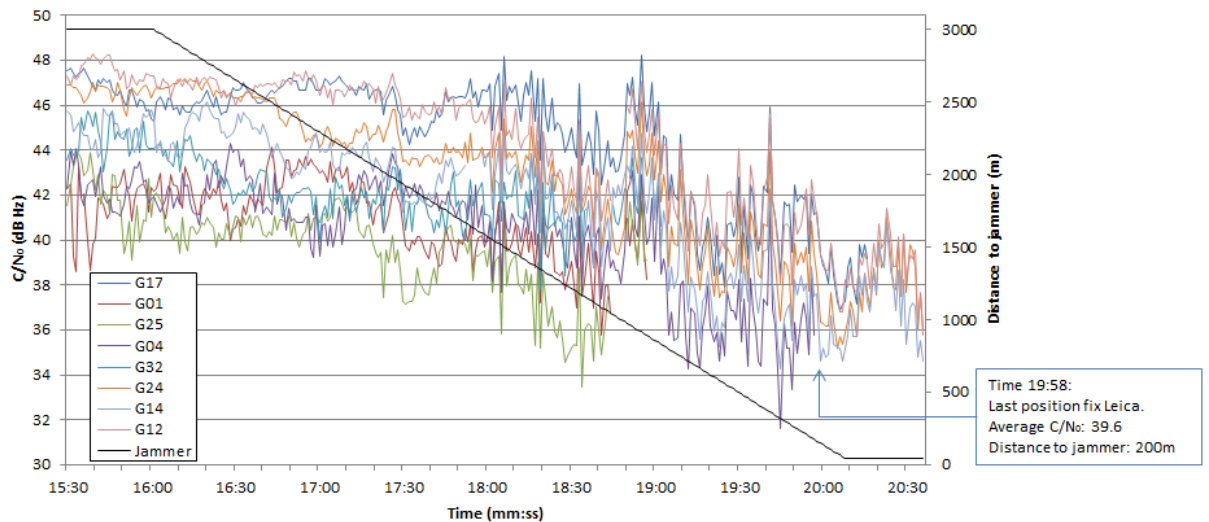


Figure 4.16: Carrier-to-noise ratios GPS satellites

The average unjammed C/N_0 is 44.8 and when the receiver lost acquisition to each particular satellite the average C/N_0 was 38.6. For the static test the average unjammed C/N_0 was 47.3 and the C/N_0 when the receiver lost acquisition was 32.7. For this dynamic test the receiver only tolerated an average fall in carrier-to-noise ratio of 6.2 dB compared to the static test where the average tolerated fall for the GPS satellites was 14.6 dB.

Because antennas for marine applications require a uniform gain pattern also below the horizon to compensate for the rolling and pitching of the ship they will be more affected by noise compared to the survey grade antennas where the gain is limited as far as possible to the upper hemisphere rejecting signals coming from below the horizon (Hofmann-Wellenhof 2008). Therefore, in addition to the dynamics of the vessel and larger multipath effect on board the vessel, the unjammed C/N_0 levels are lower than in the static test.

According to Rao et al. (2013) C/N_0 threshold levels of between 30 and 35 are acceptable for antennas on platforms that are moving, and the receiver in this test lost acquisition already when the C/N_0 descended to 38.6. However, the C/N_0 values depends on the antenna used, the receiver and the dynamics of the platform together with the setup which means that different receiver and antenna combination and cables with varying resistances show different C/N_0 patterns.

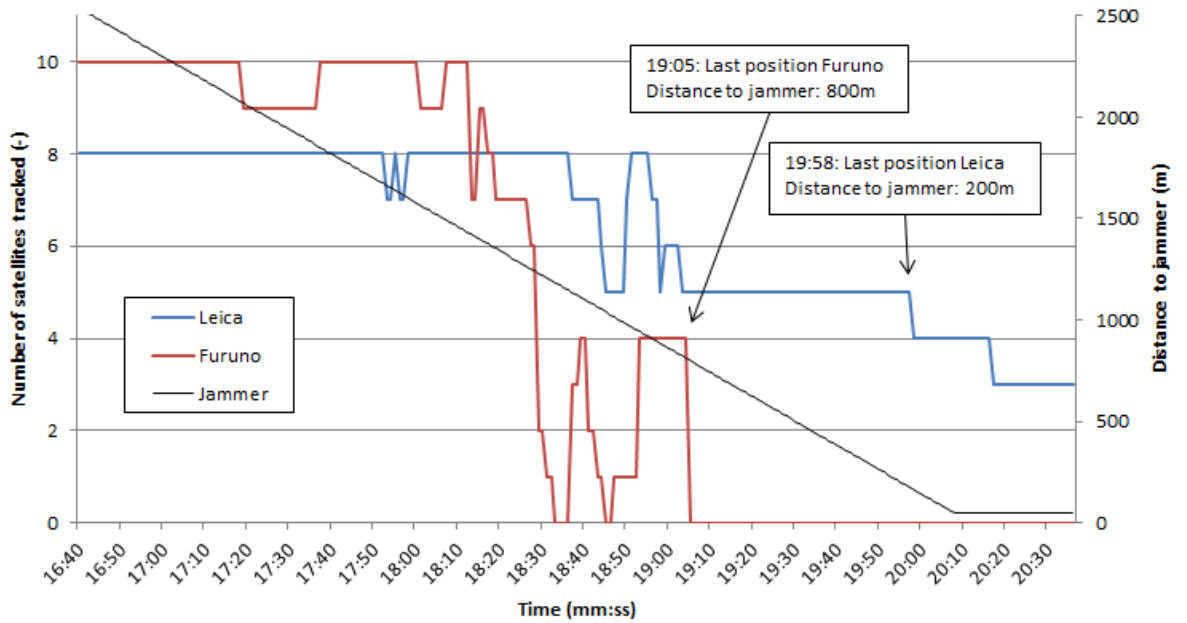


Figure 4.17: Number of GPS satellites tracked by Leica and Furuno receiver

Figure 4.17 shows the number of GPS satellites tracked by the Leica and Furuno receiver, which are connected to the same antenna. Both Figure 4.16 and 4.17 show that the last position fix for the Leica receiver occurs when the number of satellites tracked falls from 5 to 4. At that time the distance to the jammer is about 200 metres. Already at a distance of 1200 metres the Furuno receiver gives it first position gap and the position is completely lost at a distance to jammer of 800 metres. This figure shows that the Leica receiver has significantly better ability to track noisy satellites compared to the Furuno receiver.

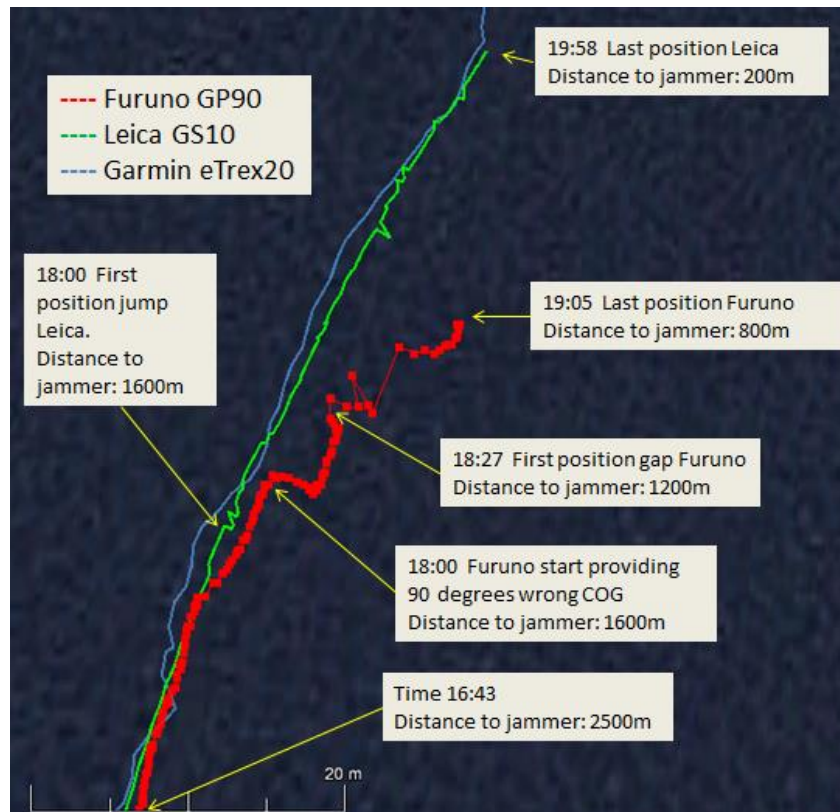


Figure 4.18: Position plot provided by the three receivers (Trial 1)

Figure 4.18 shows the position solution provided by the three receivers for the same time period as Figure 4.17. At a distance to the jammer of about 1600 metres the Furuno receiver provided a course over ground (COG) in south-eastern direction when the vessel was drifting to the north-east. As also shown in Figure 4.17 we can see the first position gaps when the distance to jammer was about 1200 metres and further that the position was completely lost at a distance of 800 metres to the jammer. At that point the difference between the Furuno and Leica position solution was about 15 metres. The Leica receiver made some smaller jump in the position during this trial, and we can see that Garmin and Leica followed almost the same track. The Leica receiver lost position when the distance to the jammer was about 200 metres. The Garmin receiver provided a consistent position with no gaps during this trial until it lost its position about 100 metres from the jammer.

Equally to the findings of Grant and colleagues (2010) the marine grade receiver started to provide significant misleading information when the jammer power was weak, already at distances of 1600 metres in this trial.

4.2.2 Trial 2: Jamming effects on the GPS receivers

In this trial the Coast Guard Vessel approached the jammer, and Figure 4.19 shows the position solution provided by the three receivers on board. The Coast Guard Vessel approached the jammer with a speed of about 5 knots (2.5 m/s). The scale in this plot is about 15 times smaller than in Figure 4.18 when the Coast Guard Vessel was drifting as shown in the lower left corner.

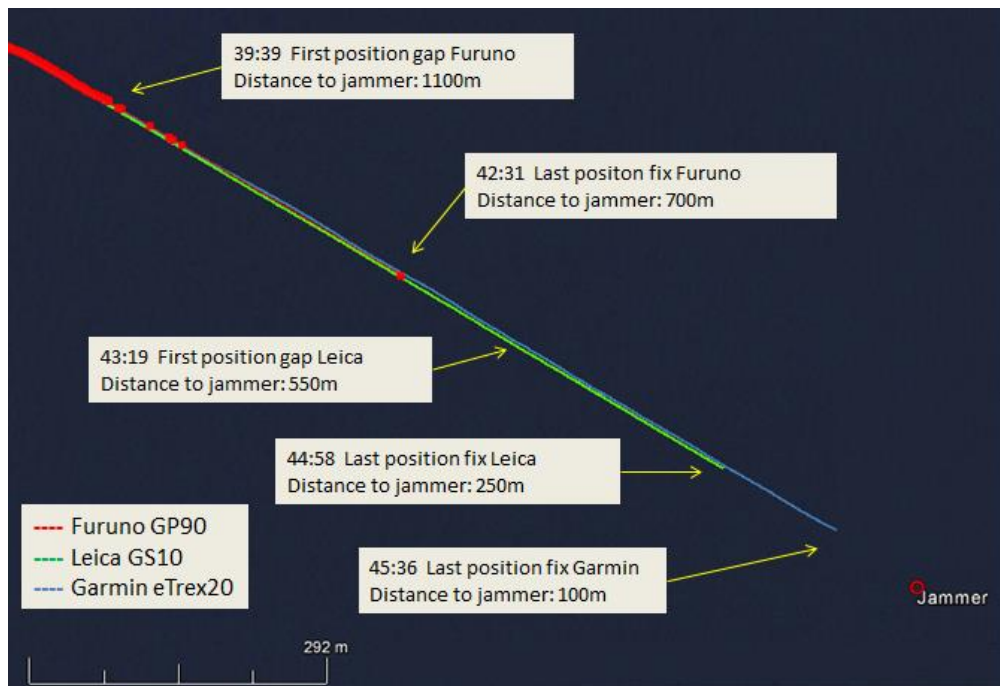


Figure 4.19: Position plot provided by the three receivers (Trial 2)

The first position gap by the Furuno receiver occurred at a distance of 1100 metres versus 550 metres for the Leica receiver. At a distance of 700 metres the Furuno receiver provided its last position versus 250 metres for the Leica receiver. The Garmin receiver provided consistent position until a distance of about 100 metres to the jammer.

In Figure 4.20 the area for the first position gap to the Furuno receiver at about 1100 metres is zoomed in. Here we can see the inconsistency of the Furuno position while the Leica and Garmin receivers provide approximate parallel position solutions in a straight line.



Figure 4.20: Position plot provided by the three receivers (Trial 2)

We have thus seen that even though the Furuno and Leica receiver are connected to the same antenna they provide significantly different position performance during these two trials.

4.2.3 Trial 2: Jamming effects on ECDIS

Figure 4.21 gives an overview of the NMEA inputs to the Electronic Chart Display and Information System (ECDIS) on board the Coast Guard Vessel.

The screenshot shows a window titled "NMEA datainnnganger (own IP:172.31.3.82)". It contains a table with the following data:

sensor	port	id	description	status
Position 1	COM 8	GGA	Gps 1	data
Position 2	IP 3	GGA	Ais	data
COG/SOG 1	COM 8	VTG	Gps 1	data
COG/SOG 2	COM 5	VDO	Ais	data
Heading 1	COM 3	HDT	Gyro	data
Heading 2	COM 5	VDO	Ais	data
Speed Log	COM 6	VHW	Log	data
Rd. Arpa 1	IP 1	TTM	Radar 1	no data
Rd. Arpa 2	IP 1	TTM	Radar 2	no data
Rd. curs.1	IP 1	RSD	Radar 1	data
Rd. curs.2	IP 1	RSD	Radar 2	data
AIS	COM 5	Absx	Ais	data
Depth	COM 9	DPT	Dybde	data
Rel. wind	COM 7	MWV	Vind	no data
Route	---	RTE	OP	no data

At the bottom of the window, there are controls: "Bruk Position 1 som primær posisjons giver" and a checked checkbox "Vis både primær og sekundær posisjon på kart".

Figure 4.21: NMEA inputs to the ECDIS

The primary position system is the Furuno GP90 receiver (GPS1) which is previously discussed in trial 1 and 2. This receiver gives also the primary COG (Course over Ground) and SOG (Speed over Ground) input. The secondary position input is the Furuno FA-150 Automatic Identification System (AIS) which has a 12-channels internal GPS receiver. The AIS provides the secondary input for COG, SOG and heading. Primary sensor for heading is the gyro compass (Raytheon Anschutz std 22), and for speed through water (STW) the only sensor is the

electromagnetic log (EM log). When the position input 1 is lost the fall back chain is set to start applying position input 2 automatically. On this ECDIS the last backup source for navigation calculations are dead reckoning (DR) based on the gyro compass and EM log. In sum the main functions which relates to plotting of the vessel's position on the ECDIS, except from the primary heading and STW, are basically dependent on the GPS.

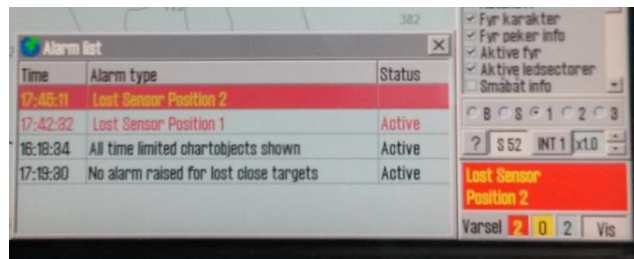


Figure 4.22: Alarm list on ECDIS

When the Coast Guard Vessel approached the jammer many alarms started to sound on the bridge. On the ECDIS screen as shown in Figure 4.22 these alarms were linked to the failure of the two GPS receivers (Position input 1 and 2) to provide position inputs, and their loss of ability to calculate SOG and COG. Alarms on the two receiver's main displays also started sounding as shown for the AIS in Figure 4.23.

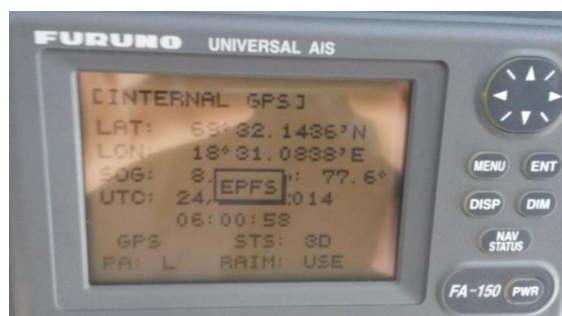


Figure 4.23: EPFS (Electronic Position Fixing System) alarm on AIS

The primary position sensor was the first sensor that was lost during this trial, and the loss occurred for the first time at a distance of 1100 metres from the jammer as shown in Figure 4.19. After that there was a large gap and a last single position fix was provided 700 metres from the jammer at time 17:42:31. As these gaps occurred the position from the secondary sensor was chosen automatically. As we can see from Figure 4.22 the alarm for lost primary position sensor was activated at time

17:42:32. This was one second after the receiver gave its last position fix. The secondary position was lost much closer to the jammer and the alarm occurred at time 17:45:11 when the distance to the jammer was about 200 metres. The integrated GPS receiver in the AIS is a less sophisticated receiver than the primary receiver, and that might be the reason why it is more resistant to jamming.

Figure 4.24 is a screenshot of the ECDIS, and we can see that there has been a jump in the position after the primary position sensor gave its last single position fix 700 metres from the jammer. Before and after that position fix the AIS provided its position input as secondary sensor.

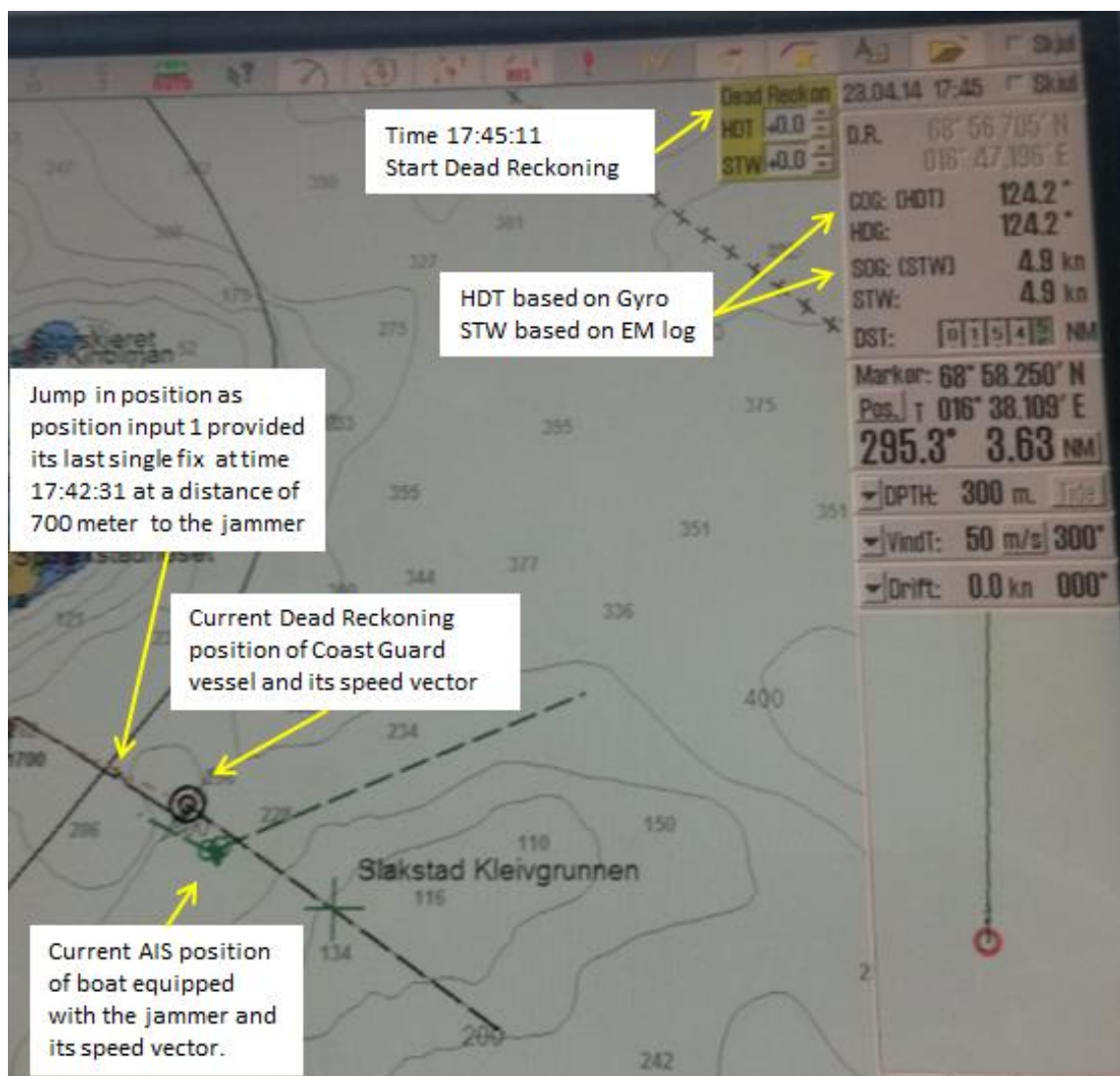


Figure 4.24: Screenshot ECDIS (Trial 2)

As soon as the secondary position sensor was lost at time 17:45:11 Dead Reckoning (DR) calculations started in the ECDIS. These calculations were based on the

heading from the gyro compass (HDT – Heading True) and speed from the EM log (STW – Speed through Water). The only notice of the start of DR positioning was the yellow squared menu that appeared in the upper right corner of the ECDIS screen. In that DR menu it was possible to set corrections to HDT and STW manually as it is necessary to adjust for biases caused by current and wind.

An important observation was that the gyro compass was equipped with automatic speed and latitude error correction that took directly input from only the primary GPS receiver. There was no operator panel or any other possibilities to enter speed and latitude manually to the gyro compass, which implies that for longer times with GPS outage the gyro errors will grow. This lack of ability to give manually latitude and speed input to the gyro is a problem that is highly recommended to be resolved.

Also the EM log was affected by errors and these errors were in order of 1 to 1.5 knots. The recommendation is to calibrate this log once a year, but there has been no routine for calibrating the EM log on board as this sensor is rarely used.

As shown in Figure 4.24 the AIS on board the small boat equipped with the jammer provided a speed vector indicating a speed of more than 10m/s. At this time this boat was dead in water.

4.2.4 Discussion

The first dynamic trial showed that the Furuno receiver provided erroneous positions data when the jammer was on a distance of 800 to 1600 metres. Until the first gap in the position that occurred when the jammer was on a distance of 1200 metres there were no indications of a wrong position or any alarms on the bridge, and there was no system that captured the difference in about 90 degrees between the COG from the primary GPS and the gyro heading. At this phase no one on the bridge took notice of the wrong position and COG that was presented on the ECDIS.

When the jammer power increased a lot of alarms started to sound simultaneously in different parts of the bridge, and most of the attention to the navigators was related to recognise and acknowledge these alarms.

The results from the first trial showed that the survey grade receiver did not provide erroneous positions to the same extent as the marine grade receiver. Instead of providing wrong positions the survey grade receiver stopped providing any position

when the interference from the jammer was high enough. When navigating this is clearly the preferred situation as providing erroneous position may lead the navigators to fail to recognise that the GPS is being interfered with. Continuation of safe navigation is dependent on the ability to recognise that the GPS service is being denied at the first stage and then operate safely using alternative navigation techniques in order to manually update the position.

As previously discussed the jamming on Pole Star led to no updating of the ECDIS which according to Grant and colleagues (2010) resulted in a static screen and further, in the Flamborough trial the ECDIS gave an alarm and closed down (ibid). Unlike these two trials discussed by Grant et al. (2010), the ECDIS in this trial provided an adequate response to loss of GPS positions as the DR system started to calculate new positions based on heading from the gyrocompass and speed from the EM log. There were alarms when the primary and secondary position sensors were lost, but no alarms that indicated that the system had started DR. Therefore some of the navigators did not recognise that the position of the vessel automatically was plotted forward, and there was also a lack of skill to manually correct the position of the vessel in DR mode as some of the navigators had never done this before.

These findings support the findings by Grant et al. (2010) who claimed that sailing in area where the jamming signals is weak is the worst situation as the navigation system might give false but plausible positions and velocities but not providing any alarms. When the vessel entered the area with higher jammer power a lot of alarms started to sound, and there were no doubt on the bridge that there was something wrong with the GPS system.

Moreover, the results have shown that the Leica and Garmin receiver have better jamming resistance and provide significantly better performance than the marine grade Furuno receiver under jamming conditions. We have also seen that the secondary position sensor on board has better jamming resistance than the primary position sensor. These findings are important for the crew to be aware of, and the Furuno GP90 receiver should not be recommended to be used in any scenarios where a jamming threat might be possible as it provide more false positions and loose its position fix at an earlier stage compared to the Leica and Garmin receiver.

5 Conclusion

This research has revealed that GPS is very vulnerable to jamming, and that different receivers react quite differently to radio frequency interference.

The research has further shown that applying the Glonass system in addition to GPS might provide benefits with regards to reliability and redundancy, especially in Northern areas. We have also seen that signals from satellites with high elevations reach the receiver antennas with higher signal strength and therefore are more resistant to a jammer on sea level. Glonass provides more satellites with higher elevation and has better coverage in Northern areas, and because it applies a different modulation technique than GPS the use of both systems would provide better redundancy.

Carrier-to-noise ratios have proven to be a good quality indicator of GNSS signals, and Glonass signals have shown to be more resistant to jamming than GPS signals as more jammer power is needed to affect the carrier-to-noise ratios. Further, the survey grade receiver has shown ability to track Glonass signals on lower carrier-to-noise ratios than GPS signals.

The static test has also showed that utilizing the Leica receiver in combined GPS + Glonass mode provides a later loss of lock and earlier acquisition when exposed to a jammer than in GPS only mode. The pseudorange precision has also appeared to be better in combined mode under difficult jamming conditions. It is worth to mention that this might be caused by the fact that the receiver in combined mode has more satellites to choose among and the better coverage of the Glonass system, not necessarily because of better jamming resistance for the Glonass signals.

Moreover, for maritime navigation a weak jamming signal seems to be more dangerous than a high powered jamming signal, since it can cause GPS receivers to give misleading information without warning. It is also important for navigators to be aware of how jammers have impact on GNSS receivers, as this to a great extent is dependent on which type of receiver that is used. It is better that the GNSS receiver stops providing data than giving a false COG and position like the Furuno receiver, which were especially shown in the first dynamic trial where the difference in COG and heading from the gyro compass was about 90 degrees.

6 Recommendations

Since this study has applied a combined GPS + Glonass receiver, further research should focus on signal reception and accuracy of a pure Glonass receiver exposed to jamming. There has been little research of jamming of the Glonass system, and because a combined receiver has been utilized in this research there are no measurements of the accuracy the Glonass system is able to provide under jamming conditions.

By looking at carrier-to-noise ratios this research showed that the GPS signals on the L2 frequency in the Leica receiver was affected to a quite similar extent as the L1 frequency by this L1 jammer. It thus seems that this dual frequency receiver is not better protected against jamming than a single frequency receiver and further studies might focus attention to this aspect.

As different receivers react quite differently to jamming, military vessels that utilize other navigation systems than the system exposed to this test should test their systems to make an assessment of its jamming resistance and further make an assessment of how their ECDIS system is able to handle a loss of position sensors. Moreover, knowledge and skills in manually correcting the ship's position in DR mode by utilizing traditional means of navigation should be attained, as this seems to be a success factor for safe navigation under jamming conditions.

7 Reference List

Axell, E., Eklöf, F., Alexandersson, M. and Johansson, P. (2013): “Jamming detection in GNSS receivers: Performance evaluation of field trials” in *Proceedings of ION GNSS 2013*, Nashville, Tennessee, September 2013.

Bauernfeind, R., Kraus, T, Dötterböck, D. and Eisfeller, B. (2011): «Car Jammers: Interference Analysis» in *GPS World*, October 2011, pp. 28-35.

Bingley, R. (2013): *Handouts Satellite Based Positioning (H24VST)*, University of Nottingham.

Borio, D.; O'Driscoll, C. and Fortuny, J., (2013): "Jammer impact on Galileo and GPS receivers," *International Conference on Localization and GNSS (ICL-GNSS)*, 25-27 June 2013 pp. 1-6, doi: 10.1109/ICL-GNSS.2013.6577265.

Burel, G. (2000): “Detection of spread spectrum transmissions using fluctuations of correlation estimators”, *IEEE-ISPACS*, Nov. 5-8, 2000, Honolulu, Hawaii.

Craven, P., Wong, R., Fedora, N., Crampton, P. (2013): *Studying the Effects of Interference on GNSS Signals. Proceedings of the 2013 International Technical Meeting of The Institute of Navigation. January 29 - 27, 2013, San Diego, California.*

Global Positioning Systems Wing (2010): *Interface specification IS-GPS-200E* [Online] Retrieved from: www.gps.gov/technical/icwg/IS-GPS-200E.pdf [28.11.13].

Grant, A., Williams, P. and Basker, S. (2010): “GPS Jamming and its impact on maritime safety” in *Port Technology International*, vol. 46, pp. 39-41.

Grant, A., Williams, P., Ward, N. and Basker, S. (2009): “GPS Jamming and the impact on maritime navigation” in *Journal of Navigation*, vol. 62, pp.173-187.

Hofmann-Wellenhof, B. (2008): *GNSS—global navigation satellite systemes: GPS, GLONASS, Galileo and more.* Wien and New York: Springer.

Jones, M. (2011): “The Civilian Battlefield. Protecting GNSS Receivers from Interference and Jamming” in *InsideGNSS* March/April 2011, pp. 40-49.

Kaplan, E. and Hegarty, C. (2006): *Understanding GPS. Principles and applications.* Norwood, MA: Artech House.

Kraus, T., Bauernfeind, R. and Eisfeller, B. (2011): “Survey of In-Car Jammers – Analysis and Modelling of the RF Signals and IF Samples” in *Proceedings of ION GNSS 2010, Portland, Oregon, Sept 2011*, pp. 430-435.

Kuusniemi, H., Airos, E., Bhuiyan, M. and Kröger, T. (2012): “GNSS Jammers: how vulnerable are Consumer grade Satellite Navigation Receivers?” in *European Journal of Navigation*, vol. 10, no. 2, pp. 14-21.

Last, D. (2010): “GNSS: The Present Imperfect” in *InsideGNSS*, May 2010, pp. 60-64.

Misra, P. and Enge, P. (2012): *Global positioning system. Signals, Measurements, and Performance.* Lincoln, Massachusetts: Ganga-Jamuna Press.

Mitch, R., Dougherty, R., Psiaki, M., Powell, S., O’Hanlon, B., Bhatti, J. and Humphreys, T. (2011): “Signal characteristics of Civil GPS Jammers” in *Proceedings of ION GNSS 2011*, pp. 20-23.

Navigation News. *The Magazine of the Royal Institute of Navigation* (2013): “Shoring Up Coastal Navigation”, Nov/Dec 2013, pp 16-17.

Niekerk, A. and Combrinck, L. (2012): “The use of civilian type GPS receivers by the military and their vulnerability to jamming” in *South African Journal of Science* vol. 108, no. 5/6, pp. 1-4.

Norwegian Space Centre (2013): “Vurdering av samfunnsmessig sårbarhet rundt bruk av globale satellitnavigasjonssystemer” [Assessment of vulnerability of infrastructure due to use of global navigation satellite systems].

Pullen, S. and Gao, G. X. (2012): "GNSS Jamming in the Name of Privacy" in InsideGNSS March/April 2012, pp. 34-43.

QinetiQ (2001): "Study into the impact on capability of UK Commercial and Domestic Services Resulting from the loss of GPS signals".

Rao, B., Kunysz, W., Fante, R., McDonald, K. (2013): GPS/GNSS Antennas. Artech House

Tong, J.R.; Watson, R and Mitchell, C (2011): "Lone sentinel: single-receiver sensitivity to RF interference.(GNSS SYSTEM)." GPS World. [online] Retrieved from: <<http://www.highbeam.com>> [24.07.14]

Vladislav V. Demyanov, Yury V. Yasyukevich and Shuanggen Jin (2013): "Effects of Solar Radio Emission and Ionospheric Irregularities on GPS/GLONASS Performance" in. Shuanggen Jin (ed.): Geodetic Sciences - Observations, Modeling and Applications. DOI: 10.5772/54568. [Online] Retrieved from: <http://www.intechopen.com/books/geodetic-sciences-observations-modeling-and-applications/effects-of-solar-radio-emission-and-ionospheric-irregularities-on-gps-glonass-performance> [21.09.14]

Volpe, J. (2001): "Vulnerability assessment of the transportation infrastructure relying on the global positioning system" National Transportation Systems Center, Final report.

Ward, P. (1994): "GPS Receiver RF Interference Monitoring, Mitigation, and Analysis Techniques" in sNavigation-Journal of the Institute of Navigation, Vol. 41, No. 4, Winter 1994.

Appendices

Appendix A: Specifications Leica GS10 and AS10

GNSS technology	Leica patented SmartTrack+ technology: <ul style="list-style-type: none"> • Advanced measurement engine • Jamming resistant measurements • High precision pulse aperture multipath correlator for pseudorange measurements • Excellent low elevation tracking • Very low noise GNSS carrier phase measurements with <0.5 mm precision • Minimum acquisition time 	
No. of channels	120 channels	
Max. simultaneous tracked satellites	Up to 60 Satellites simultaneously on two frequencies	
Satellite signals tracking	<ul style="list-style-type: none"> • GPS: L1, L2, L2C, L5 • GLONASS: L1, L2 • Galileo (Test): GIOVE-A, GIOVE-B • Galileo: E1, E5a, E5b, Alt-BOC • BeiDou: B1, B2 • SBAS: WAAS, EGNOS, GAGAN, MSAS 	
GNSS measurements	Fully independent code and phase measurements of all frequencies <ul style="list-style-type: none"> • GPS: carrier phase full wave length, Code (C/A, P, C Code) • GLONASS: carrier phase full wave length, Code (C/A, P narrow Code) • Galileo: carrier phase full wave length, Code • BeiDou: carrier phase full wave length, Code 	
Reacquisition time	< 1 sec	
Standard survey antennas		
Types	AS10	AS05
GNSS technology	SmartTrack+	SmartTrack
Satellite signal tracking	GPS: L1, L2, L5 GLONASS, Galileo, BeiDou	GPS: L1 GLONASS, BeiDou: B1
Ground plane	Built-In Ground plane	Built-In Ground plane
Dimensions (diameter x height)	170 mm x 62 mm	170 mm x 62 mm
Weight	0.44 kg	0.44 kg
Gain	29±3 dbi	Typically 27 dbi
Temperature operating / storage	-40° C to +70° C / -55° C to +85° C	
Humidity	100%	
Protection against water, sand	IP68 according IEC60529 and MIL STD 810F - 506.4-I, MIL STD 810F - 510.4-I and MIL STD 810F - 512.4-I	
Drops & topple over	Withstands 1.5 m drop onto hard surfaces and survives topple over from a 2 m pole onto hard surfaces	
Vibration	Withstands vibrations during operation on large civil construction machines Compliance with ISO9022-36-08 and MIL-STD 810F - 514.5-Cat24	

(Extracted from: www.leica-geosystems.com)

Appendix B: Specifications Furuno GP90

SPECIFICATIONS OF GP-90

GPS

Receiver	12 discrete channels all-in-view, C/A code
RX Frequency	L1 (1575.42 MHz)
Time to First Fix	12 s (Warm start)
Tracking Velocity	900 kt
Geodetic System	WGS-84 (NAD-27 or others selectable)
Update Rate	1 s

Positioning Augmentation

DGPS

Reference Station:	Automatic or manual selection
Frequency Range:	283.5 - 325.0 kHz (all ITU regions)
Format:	RTCM SC-104 Ver 2.0 Type1, 7, 9, 16

WAAS

Standard fitted in display unit

Accuracy

GPS:	10 m (95%)
DGPS:	5 m (95%)
WAAS:	3 m (95%), limited coverage
SOG:	±0.001 kt (calm sea)
COG:	±3° (SOG 1-17 kt), ±1° (SOG > 17 kt)

Display

6" LCD (120 W, 91 H mm), 320 (H) x 240 (V) pixels, L/L resolution: 0.001 min
--

Display Modes

VideoPlotter, Highway, Text, Steering

VideoPlotter

Scale:	0.02 to 320.0 nm,
Plot Interval:	1 s - 60 min or 0.01-99.99 nm

Memory Capacity

2,000 points for ship's track and marks, 999 waypoints with comments, 30 routes (containing 30 waypoints/route)

Alarms

Arrival, anchor watch, XTE, speed, time, water depth, trip, DGPS, WAAS

Integrity indication

Safe, Caution, Unsafe at accuracy level of 10 m or 100 m

Interface (IEC 61162-1 Ed 2, NMEA 0183):

Output GBS (satellite fault), GLL (L/L), VTG (SOG, COG), ZDA(UTC), WPL (WPT location), etc.

Input DBT (Depth), HDT (Compass), MTW (Water temperature), TLL (TGT L/L), VBW (Dual grd/wat spd), etc.

ENVIRONMENT (IEC 60945 test method)

Temperature	Display Unit: -15°C to +55°C Antenna Unit: -25°C to +70°C
Waterproofing	Display Unit: IPX5 (IEC 60529), CFR46 (USCG) Antenna Unit: IPX6 (IEC 60529)
EMC	IEC 60945 Ed. 4 (up to 2 GHz)

POWER SUPPLY

12-24 VDC, 0.8-0.4 A

EQUIPMENT LIST

Standard

1. Display Unit (Specify single or dual)	1 unit
2. Antenna Unit GPA-017S	1 unit
3. Antenna Cable	15 m
4. Interface Cable	5 m x 2 pcs
5. Installation Materials and Spare Parts	1 set

Option

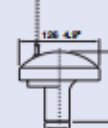
- DGPS Receiver Kit OP20-32-1/20-33
- Whip Antenna FAW-1.2 for GPA-018S
- Antenna Cable, 30/50 m
- Interface Cable, 5/10 m
- Antenna Base
CP20-01111 (Pipe mount), No.13-QA300 (Deck mount)
No.13-QA310 (Offset bracket), No.13-RC5160 (Handrail mount)
- Flush Mount Kit OP20-24/20-25
- Interface Unit IF-2500
- External DGPS Receiver GR-80
- Rectifier PR-62

Antenna Unit

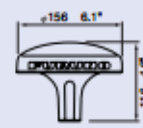
GPA-017S
0.15 kg 0.3 lb



GPA-018S
0.3 kg 0.7 lb

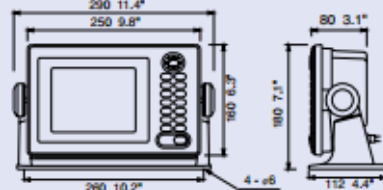


GPA-019S
1.0 kg 2.2 lb



Display Unit

2.2 kg 4.9 lb



(Extracted from: www.furuno.com/en)